

# Understanding the Wheel/Rail Transfer Mechanism in Liquid Friction Modifier Carry-down

by

Morgan John Edwin Hibbert

B.A.Sc., The University of British Columbia, 2010

A THESIS SUBMITTED IN PARTIAL FULFILLMENT OF  
THE REQUIREMENTS FOR THE DEGREE OF  
MASTER OF APPLIED SCIENCE

in

The Faculty of Graduate and Postdoctoral Studies  
(Mechanical Engineering)

THE UNIVERSITY OF BRITISH COLUMBIA  
(Vancouver)

April 2017

© Morgan John Edwin Hibbert 2017

# Abstract

In the rail road industry liquid friction modifiers (LFM's) are used on the top of rail (TOR) between the wheel/rail interface to reduce curve noise, lateral forces, rail wear and fuel consumption. The friction modifier may be applied to the rail via a track side applicator and is carried down by the train into curved sections of the track where the greatest benefit is seen.

A custom laboratory scale machine was designed and built for the purpose of conducting experiments to study the behaviour of LFM carry-down over a large number of wheel/rail interactions. The machine was also designed so that the film transfer at the wheel/rail interaction location could be studied.

The use of a fluorescent agent to enhance the ability to visualize LFM carry-down showed promising results, enabling small amounts of carry-down that couldn't otherwise be seen under ambient light conditions to now be seen under fluorescence.

Qualitative experiments using the machine were performed showing that an increase in the wheel speed results in an increase in the amount of friction modifier transferred from the rail to the wheel at the initial pickup location, thus increasing the carry-down. Increasing the applied load had the opposite effect and reduced the amount of friction modifier initially transferred from the rail to the wheel, and thus reducing the carry-down. The profile of the wheel was observed to effect the initial transfer amount and the ensuing carry-down due to high/low pressure zones along the wheel/rail interface.

# Preface

The authors of chapter 2 are Morgan Hibbert, Dr. Sheldon Green and representatives from L.B. Foster. Dr. Sheldon Green and representatives from L.B. Foster provided input and suggestions that shaped the final design of the machine.

The authors of chapter 3 are Morgan Hibbert, Dr. Sheldon Green and Hatef Rahmani. Dr. Sheldon Green proposed methodologies to help visualize KELTRACK®. Hatef Rahmani ran shear stress and shear viscosity tests on the KELTRACK® product.

The authors of chapter 4 are Morgan Hibbert and Dr. Sheldon Green. Dr. Sheldon Green helped to guide the experiments that were chosen and how they were conducted.

The authors of chapter 5 are Morgan Hibbert and Dr. Sheldon Green. Dr. Sheldon Green provided analysis and possible explanations for the results seen in the experiments.

# Table of Contents

<b>Abstract</b> . . . . .	ii
<b>Preface</b> . . . . .	iii
<b>Table of Contents</b> . . . . .	iv
<b>List of Tables</b> . . . . .	vi
<b>List of Figures</b> . . . . .	vii
<b>Acknowledgements</b> . . . . .	ix
<b>Dedication</b> . . . . .	x
<b>1 Introduction</b> . . . . .	1
1.1 Background . . . . .	1
1.2 Initial Research Questions and Previous Work . . . . .	1
1.3 Final Research Objectives . . . . .	3
<b>2 Machine Design</b> . . . . .	4
2.1 Experimental Needs & Motivation . . . . .	4
2.2 Components . . . . .	5
2.2.1 Overview . . . . .	5
2.2.2 Wheel/Rail Interaction Location . . . . .	7
2.2.3 Wheel Design . . . . .	10
2.2.4 Force Generation & Control . . . . .	12
2.2.5 Motor Control . . . . .	14
2.2.6 DAQ Interface . . . . .	15
2.2.7 Software Controller . . . . .	16
2.2.8 Measurement Sensors . . . . .	17
2.3 Capabilities . . . . .	18

*Table of Contents*

---

<b>3</b>	<b>Methods</b>	20
3.1	Application of KELTRACK®	20
3.2	Fluorescent Additive	21
3.3	Control of Speed and Pressure	24
3.4	Experimental Operation	25
<b>4</b>	<b>Experiments &amp; Results</b>	27
4.1	Initial LFM Carry-down Experiments	27
4.2	Long Term LFM Carry-down Experiment	34
4.3	Effect of Speed on LFM Carry-down	43
4.4	Effect of Pressure on LFM Carry-down	54
<b>5</b>	<b>Discussion of Results</b>	61
5.1	Initial LFM Carry-down Experiments Discussion	61
5.2	Long Term LFM Carry-down Experiment Discussion	63
5.3	Effect of Speed on LFM Carry-down Discussion	64
5.4	Effect of Pressure on LFM Carry-down Discussion	67
<b>6</b>	<b>Conclusion</b>	68
6.1	Recommended Changes to Machine	70
	<b>Bibliography</b>	71
 <b>Appendices</b>		
<b>A</b>	<b>Experimental Procedure</b>	73
A.1	Pre Run Checklist	73
A.2	Test Procedure	73
A.3	Normal Shut Down Procedure	74
<b>B</b>	<b>Hertzian Contact Patch Calculations</b>	75
<b>C</b>	<b>Control Circuitry Schematic</b>	77

# List of Tables

2.1	Machine capabilities...	19
4.1	Long term carry-down conditions...	34
4.2	Long term carry-down observation stages...	35
4.3	Effect of speed test conditions...	43
4.4	Effect of pressure test conditions...	54
5.1	Long term carry-down observation stages, scaled...	64

# List of Figures

2.1	Wheel/rail transfer machine . . . . .	6
2.2	Wheel/rail interaction location, front view. . . . .	7
2.3	Wheel/rail interaction location, rear view. . . . .	8
2.4	Wheel design . . . . .	10
2.5	Force control . . . . .	12
2.6	Motor control . . . . .	14
2.7	DAQ interface . . . . .	15
2.8	Software controller . . . . .	16
2.9	Measurement sensors . . . . .	17
3.1	KELTRACK® application method . . . . .	21
3.2	Rhodamine-B excitation and emission spectra . . . . .	22
3.3	Rhodamine-B detection schematic . . . . .	22
3.4	KELTRACK® Rhodamine-B shear test results . . . . .	23
3.5	KELTRACK® Rhodamine-B fluorescence test . . . . .	24
3.6	Photo diode trigger sensor . . . . .	26
4.1	Initial carry-down: Interaction #0 . . . . .	28
4.2	Scratches on wheel . . . . .	29
4.3	Initial carry-down: Interaction #1 & #3 . . . . .	30
4.4	Initial carry-down: Interaction #5 & wheel . . . . .	31
4.5	Initial carry-down: Pressure profile . . . . .	32
4.6	Film splitting . . . . .	33
4.7	Long term carry-down: Initial application of dried KELTRACK® . . . . .	36
4.8	Long term carry-down: Comparison of KELTRACK® on wheel . . . . .	37
4.9	Long term carry-down: Wheel after the experiment . . . . .	38
4.10	Long term carry-down: KELTRACK® transfer 1 . . . . .	39
4.11	Long term carry-down: KELTRACK® transfer 2 . . . . .	40
4.12	Long term carry-down: KELTRACK® transfer 3 . . . . .	41
4.13	Long term carry-down: KELTRACK® transfer 4 . . . . .	42
4.14	Effect of speed: Repeatability, manual speed, ambient light . . . . .	44
4.15	Effect of speed: Repeatability, manual speed, fluorescence . . . . .	45

*List of Figures*

---

4.16	Effect of speed: Repeatability, 8 m/s, ambient light . . . . .	46
4.17	Effect of speed: Repeatability, 8 m/s, fluorescence . . . . .	47
4.18	Effect of speed: Interaction #0, ambient light . . . . .	48
4.19	Effect of speed: Interaction #0, fluorescence . . . . .	49
4.20	Effect of speed: Interaction #1 . . . . .	50
4.21	Effect of speed: Interaction #3 . . . . .	51
4.22	Effect of speed: Interaction #5 . . . . .	52
4.23	Effect of speed: Wheel . . . . .	53
4.24	Effect of pressure: Interaction #0, ambient light . . . . .	55
4.25	Effect of pressure: Interaction #0, fluorescence . . . . .	56
4.26	Effect of pressure: Interaction #1 . . . . .	57
4.27	Effect of pressure: Interaction #3 . . . . .	58
4.28	Effect of pressure: Interaction #5 . . . . .	59
4.29	Effect of pressure: Wheel . . . . .	60
5.1	Wheel/rail contact in straight/curve track . . . . .	62
5.2	Hydrodynamic fluid lubrication . . . . .	65
B.1	Hertzian contact model schematic . . . . .	75
C.1	Op amp schematic . . . . .	77

# Acknowledgements

I would like to thank my supervisor, Dr. Sheldon Green. His knowledge, guidance and experience was invaluable in carefully guiding this research towards its conclusion. I also wish to thank Dr. Green for his never ending support during my time with regards to this project and also my personal endeavours in life. He took a chance on me, and I am forever grateful that he did and to have had the blessed opportunity to work with him and learn from him.

I would like to thank L.B. Foster and NSERC for the support of this research. I would like to thank Mr. John Cotter, Dr. Louisa Stanlake, Dr. Richard Stock and Dr. Dmitry Gutsulyak.

A special thank you to Mr. David Elvidge and Mr. Joel VanderMarel who provided critical guidance and a wealth of knowledge in regards to the final design of the machine.

I would like to thank Greg Parsons and Markus Fengler from the UBC machine shop for helping me so often when it came to making and designing all the custom parts of this machine that I had to make.

I would like to thank Sean Buxton for all the help in making the high voltage components for the motor control and all the electronics advice.

# Dedication

I would like to thank Chris and Christine, Keeley, Rena and Finch for their continued support in my life journey. Without their love and support I wouldn't be where I am now.

# Chapter 1

## Introduction

### 1.1 Background

Top of rail (TOR) friction control is widely implemented in heavy haul rail environments all over the world [18], including Canadian rail road which consists of over 72,000 km of track and transports more than 270 million tonnes of freight annually [3]. This top of rail (TOR) friction control has shown benefits in reducing curve noise, lateral forces, and rail wear in freight rail systems [2, 7, 8, 10, 15]. Liquid friction modifiers (LFM's) applied to the top of rail by trackside applicators have been tested extensively on North American Heavy haul railway and field trials of these LFM's have also shown that coating the rail surface reduces fuel consumption by 6-9% [3, 4, 6, 19].

One such LFM is KELTRACK®, a non-Newtonian water-based suspension developed by Kelsan Technological Corporation (now a part of L.B. Foster). KELTRACK® is applied to the rail as a wet film by a trackside applicator ahead of the approaching train, the wheels then pick up the product via film splitting [5]. The frictional benefits of KELTRACK® is then carried down (what will be referred to as carry-down) the rail via the coated wheel [9]. It is ideal to have a trackside applicator located before a curved section of the track where the greatest need for a friction modifier exists [13].

### 1.2 Initial Research Questions and Previous Work

The carry-down mechanism of a liquid friction modifier by continuous wheel/rail interactions has been previously studied but is not yet well understood [1, 20]. Additionally there has only been a small amount of research looking into the LFM's interaction with other substances in the third body layer<sup>1</sup> between the wheel and rail [9]. A better understanding of the carry-down behaviour of KELTRACK® could be a great benefit in optimizing the process of using this LFM and for better qualifying the frictional benefits of using this product. This led to several initially proposed research questions:

## 1.2. Initial Research Questions and Previous Work

---

- After KELTRACK® is applied to the wheel, over what distance do we continue to see frictional benefits (carry-down)?
- What is the importance of dry film transfer from wheel to rail?
- What are the influences of vertical load on carry-down?
- What are the influences of the material's physical characteristics (ie cohesion/adhesion, surface wettability) on carry-down?
- What is the influence of the constituents of the existing third body layer on carry-down?
- Can a general model be developed?

Some initial research into carry-down had been conducted by L.B. Foster using an apparatus that consists of a ramp with a steel roller that is released from a certain height and rolls through a patch of wet friction modifier at the base of the ramp [16]. The results from this were not very conclusive and the apparatus had several drawbacks. It was not easy to control the speed of the wheel or the applied load on the wheel, creep<sup>2</sup> could not be simulated and only one carry-down interaction could be simulated. Further, the results that were obtained did not align with what was seen in the field.

A second apparatus called a twin-disc machine has also previously been used to conduct wheel/rail interaction experiments. It has several benefits, including independent speed control for each wheel (providing the ability to simulate creep) as well as controlling the applied load. Some drawbacks with this machine is that it uses two discs for contact instead of the disc/plane contact geometry that is seen in the field. The discs on the available machines have a radii of 25 mm, much smaller than the size of a full scale train wheel (460 mm). This size difference could potentially lead to scaling errors explaining why the laboratory results didn't match what is seen in the field. The two discs also are the same radii limiting the ability to perform carry-down experiments with clean (no previous LFM transfer) sections of simulated rail.

---

<sup>1</sup>At the interface of wheel and rail resides an intermediate layer comprised of wear particles (from wheel or rail wear) and contaminants (leaves, water, sand and oil for example). This is the third body layer.

<sup>2</sup>Creep is a term commonly used in the rail industry when the tangential velocity of the contact surface of the wheel is different than the translational velocity of the wheel. Creep occurs when the train wheel is sliding.

It was assessed that neither of these two apparatuses provided the necessary functional capabilities for running experiments that would lead to a better understanding of carry-down.

### **1.3 Final Research Objectives**

To better understand the effect of carry-down we need to be able to simulate multiple wheel/rail interactions as it is desired that the LFM provide frictional benefits for up to 6 km (~2,000 wheel/rail interactions). The two known apparatuses described earlier were deemed inadequate, therefore in order to answer the research questions posed a new machine needs to be designed that is capable of performing the required operations that will provide further insight into LFM carry-down.

The principal objective of this research was to design and build a new machine capable of answering questions about LFM carry-down. The secondary objective was to run some early qualitative experiments to validate the machines capabilities and provide some base level understanding into carry-down that will guide future research in this field.

# Chapter 2

## Machine Design

### 2.1 Experimental Needs & Motivation

The motivation behind the design of this machine is based on a combination of controllable variables that are required in order to better understand product carry-down as a result of wheel/rail interaction. No known machine currently exists that meets all these requirements and thus the need to design such a machine was presented. The main identified needs were developed in conjunction with L.B. Foster [17] and are listed below:

1. Need to replicate the speeds seen in a full scale train operation. The product is used on rail where the train will reach speeds of 70 km/h ( $\sim 19$  m/s) on straight track and 56 km/h ( $\sim 16$  m/s) in curved sections.
2. Need to replicate full scale wheel load. Contact pressures at the wheel/rail interface can be expected to reach  $\sim 1100$  MPa.
3. The laboratory experimental results need to scale and match the results seen by a full scale train in the field.
4. Wheel and rail need independent speed control so that creep can be simulated.
5. Desired to have several wheel/rail interactions where the wheel interacts with a new piece of rail (more akin to what is seen in the field). Previous set-ups had only simulated one wheel/rail interaction.
6. Line of sight access at the wheel/rail interaction location to observe the interaction.
7. Desired to simulate up to 6 km of wheel/rail interactions.
8. Repeatable process for applying the material to the wheel/rail.
9. Desired to simulate wet film transfer and dry film transfer.
10. Quantify the amount of product on the wheel/rail.

## **2.2 Components**

### **2.2.1 Overview**

An overview of the machine is presented in Figure 2.1. The cut out sections “Wheel/Rail Interaction Location” and “Pressure Control” are presented in later sections. A description of all the items is listed below.

## 2.2. Components

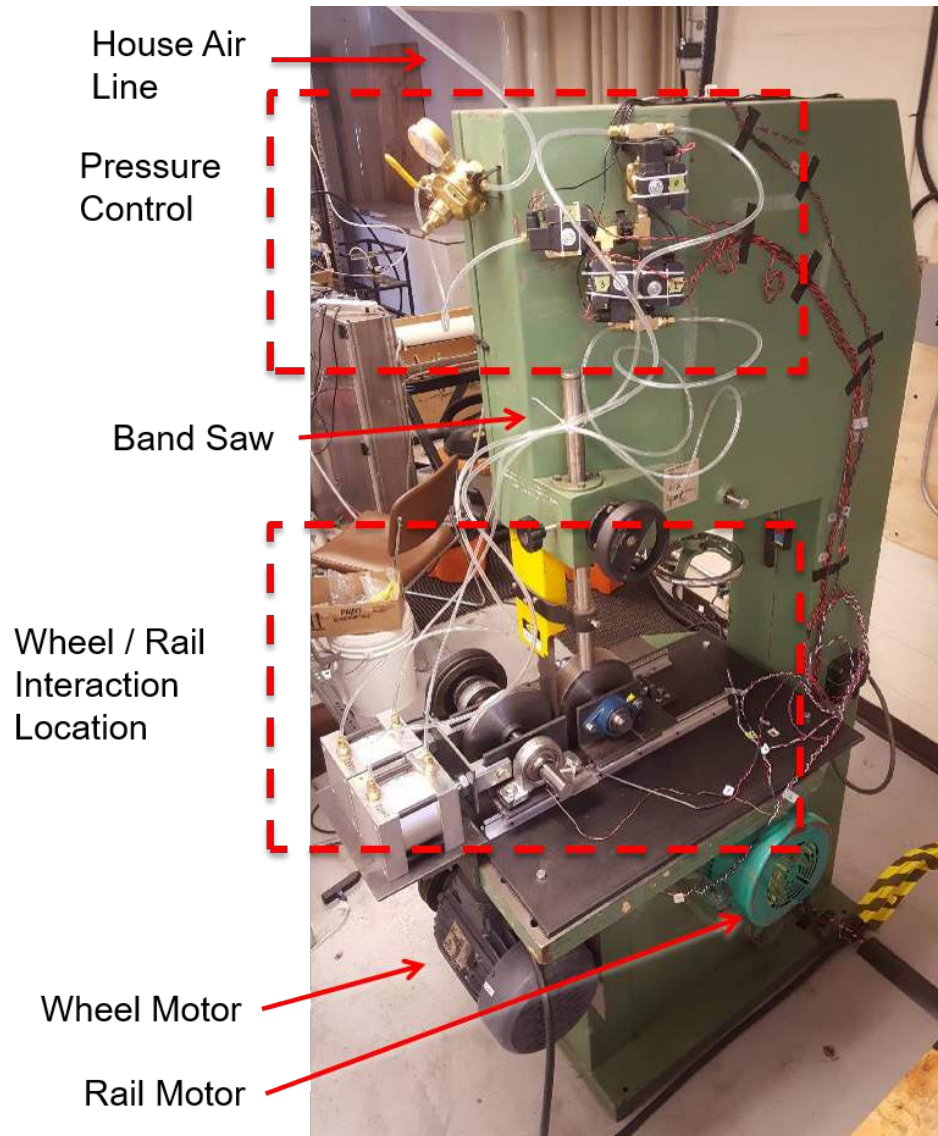


Figure 2.1: Wheel/rail transfer machine.

- **Band saw:** The machine is built on an industrial scale woodworking band saw that has been heavily modified. The original band saw was an HB-600 woodworking band saw made by General Industrial. The band saw was chosen as the base of the machine because of the long continuous moving flat metal surface of the blade that could represent

## 2.2. Components

---

the rail.

- **Wheel Motor:** This motor was added to the machine to drive the wheel independently of the rail. It is a 5 hp, 1800 rpm, 3 phase 208 V motor. This motor was selected because it could provide the speeds required.
- **Rail Motor:** This is the motor supplied with the band saw. It is a 7.5 hp, 3490 rpm, 3 phase 208 V motor.
- **House Air Line:** Air pressure is supplied by a 120 psi house air line. This air line was already installed and available at the installation location.
- **Pressure Control:** See corresponding subsection.
- **Wheel/Rail Interaction Location:** See corresponding subsection.

### 2.2.2 Wheel/Rail Interaction Location

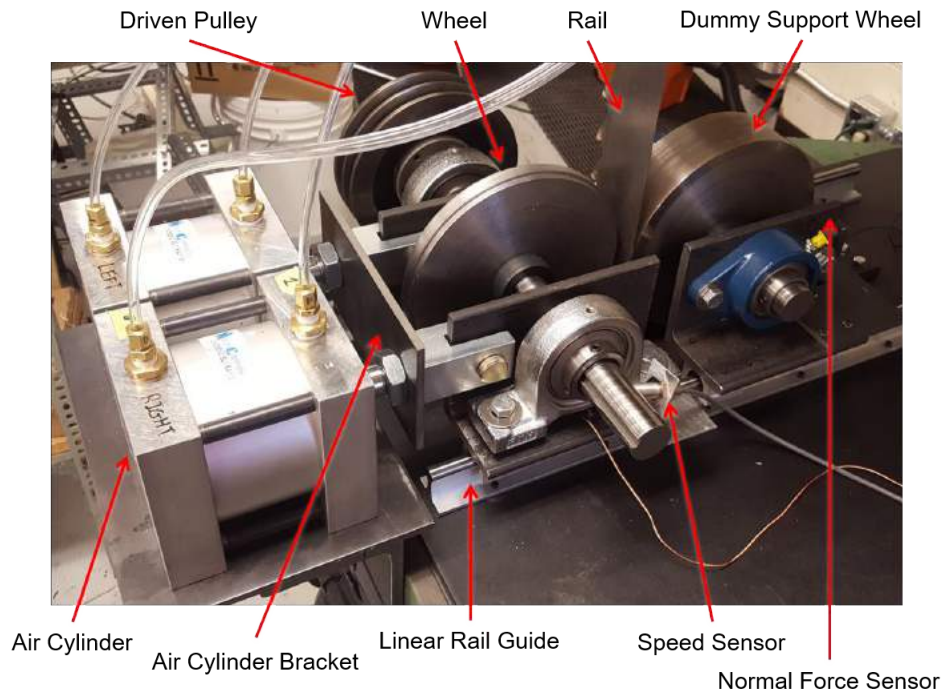


Figure 2.2: Wheel/rail interaction location, front view.

## 2.2. Components

---

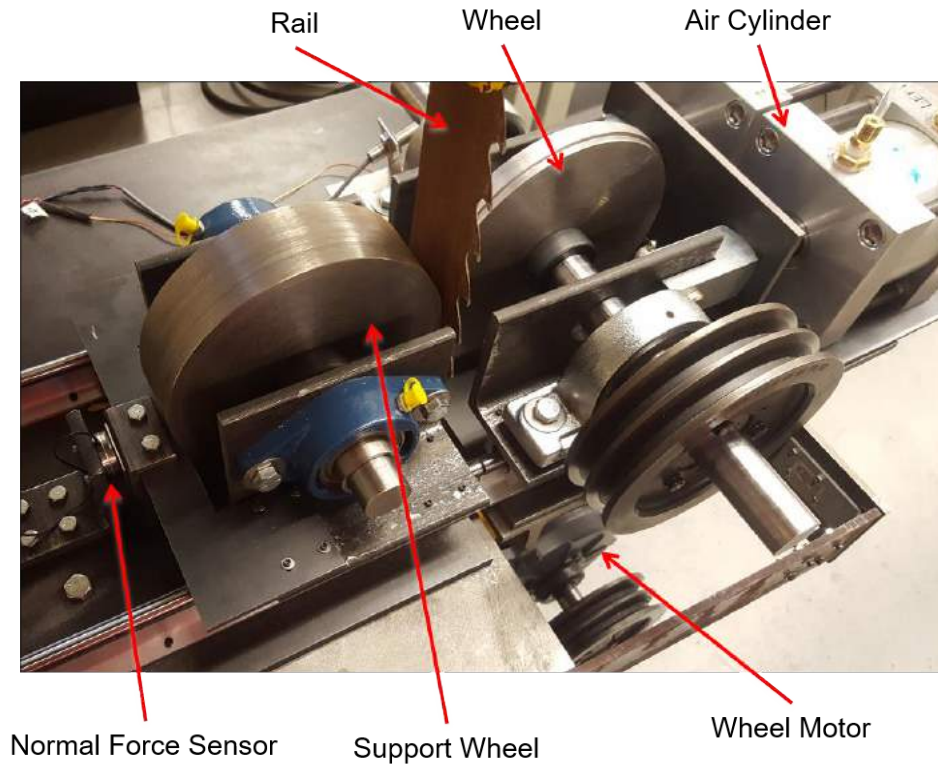


Figure 2.3: Wheel/rail interaction location, rear view.

The wheel/rail interaction location is the primary point of interest during the experiments. Figures 2.2 and 2.3 show this location and the immediately surrounding components.

- **Wheel:** This is the driving wheel, which represents the train wheel in the experiments. It is made from c1045 hot rolled steel. Details of the wheel design are described in the following section.
- **Rail:** The band saw blade represents the rail in these experiments. The blade is made of carbon steel and is 0.9 mm thick.
- **Dummy Support Wheel:** This wheel is not driven and provides a firm surface behind the rail at the wheel/rail interaction. It also serves as a conduit to the normal force sensor for measuring the applied load at the wheel/rail interface. It is made from c1045 hot rolled steel.

## 2.2. Components

---

- **Air Cylinder:** Two sensor ready tie rod air cylinders (double acting, 4-1/2" bore size, 5-1/8" wide with a 1" stroke length) are used to simulate the load at the wheel/rail interface. Each cylinder is capable of generating 1,590 lbf at 100 psi, which is enough force reach full pressure at the wheel / rail interface.
- **Air Cylinder Bracket:** The two pistons had slightly different actuation rates. To mitigate this, a bracket was installed tying the two piston rods together.
- **Linear Rail Guide:** The brackets supporting the driving wheel and the dummy support wheel are both mounted on a stainless steel linear rail guide to allow for smooth actuation and retraction of the driving wheel.
- **Speed Sensor:** A magnetic Hall effect sensor measures the speed of the wheel via the notch in the driving shaft. An identical sensor (not shown) measures the speed of the band saw wheel driving the rail (band saw blade).
- **Normal Force Sensor:** A 2000 lbf force load cell measures the normal force at the wheel/rail contact patch. More information on page 18.
- **Driven Pulley:** A double sheaved steel pulley for use with v-belts is used as part of the drive train to connect the wheel motor to the wheel shaft. V-belts were chosen because the system was easier to implement than a toothed belt but provided better force transfer than a flat belt.
- **Wheel Motor:** This motor was added to the machine to drive the wheel independently of the rail. It is a 5 hp, 1800 rpm, 3 phase 208 V motor.

### 2.2.3 Wheel Design

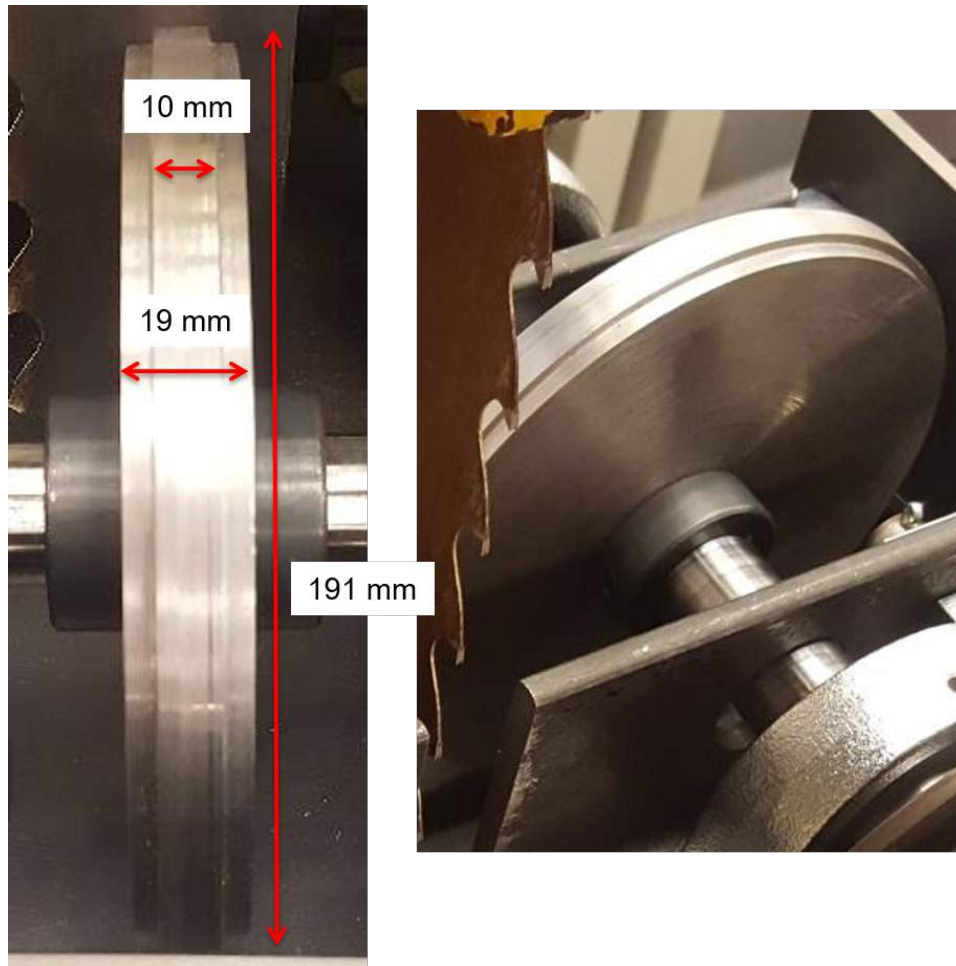


Figure 2.4: Wheel design.

The train wheel is shown in Figure 2.4. The design is based on the work done by Naeimi et al. [12] who used FE models and numerical simulation to show that a 1/5 scale model of a train wheel under scaled loading conditions can achieve the contact stresses similar to what is seen in a full scale train wheel. This formed the starting point for the design of the wheel in this machine. The final wheel design chosen was approximately 1/5 of a full scale wheel. A 1/5 wheel thickness would be 27 mm, however, an actual train wheel has a specific profile shape that is not trued with respect

## 2.2. Components

---

to the axis of rotation (Figure 5.1 shows an example of this wheel profile) and to maintain this specific shape during early experiments to maintain consistency would require constant resurfacing of the wheel as it wears during experiments. This would be an expensive and timely process, so it was decided for simplicity to start with a flat profile that is trued with the shaft axis. Using a Hertzian contact stress approximation (see Appendix B) it was found that a width of 10 mm would produce a contact pressure up to  $\sim 1000$  MPa at the wheel/rail interaction location, providing the required pressure range for the experiments. The wheel was made from a 19 mm wide disc (for added stability) with a 10 mm wide contact surface extending out.

## 2.2. Components

### 2.2.4 Force Generation & Control

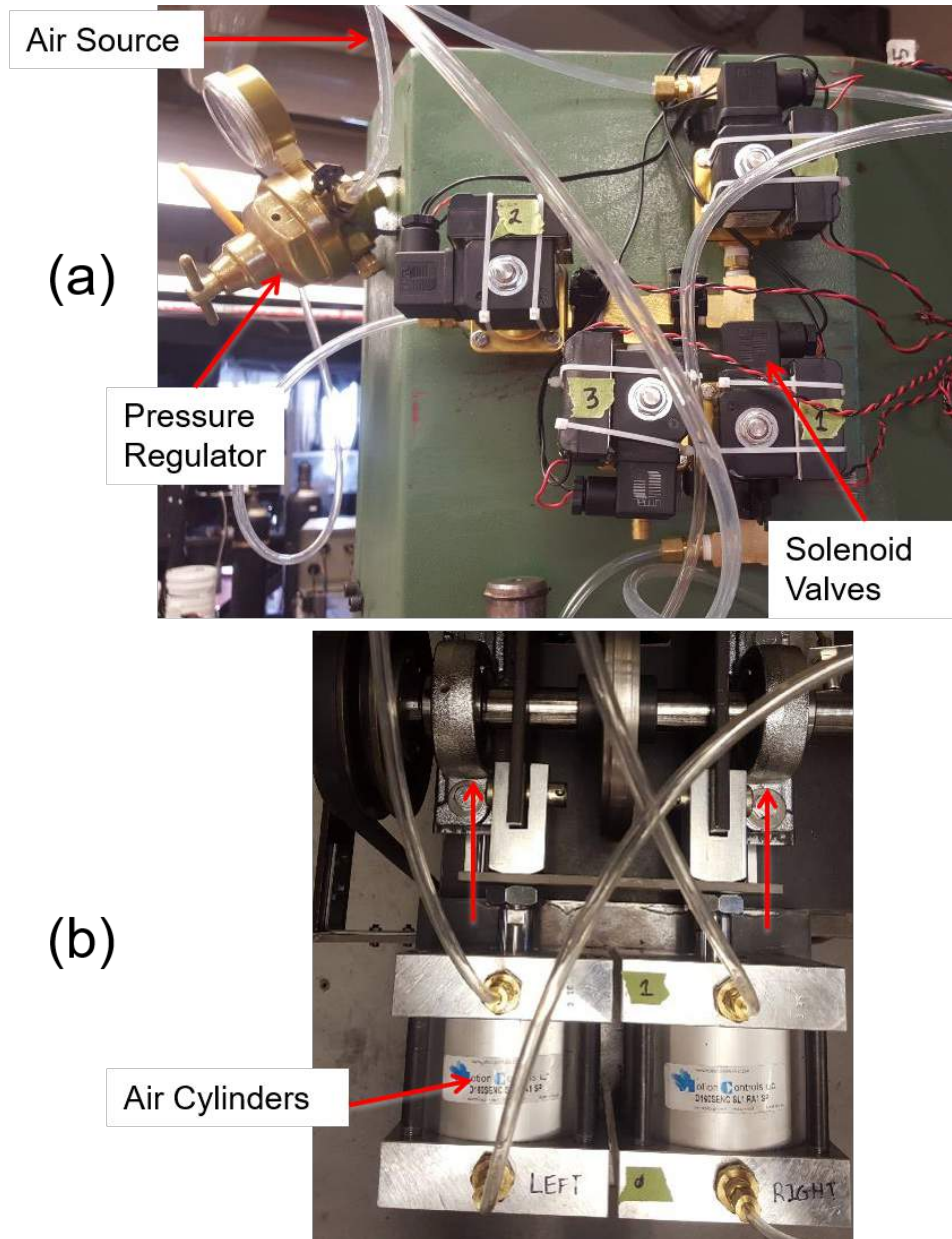


Figure 2.5: Force control: (a) Pressure direction management. (b) Force generating air cylinders.

## 2.2. Components

---

Force generation at the wheel/rail interface and the control of this actuation is done using the pneumatic system shown in Figure 2.5 and described below. A pneumatic system was chosen because of the house air line that was already available at the installation site made this the easiest to implement solution.

- **Air Source:** Air is supplied by a house air line capable of providing up to 120 psi of continuous air pressure.
- **Pressure Regulator:** 0 - 200 psi line regulator with manual control. This was chosen because of the low cost and ease of implementation.
- **Solenoid Valves:** Four normally closed, 24 V DC brass actuated solenoid valves with a 0 - 200 psi pressure rating. Each solenoid uses a solid state relay to control and drive the state of the solenoid valve. These solenoids control the direction of air flow and were chosen because of their fast acting response and ability to actuate without a pressure difference.
- **Air Cylinders:** Two double acting linear tie rod air cylinders are used for force generation at the wheel/rail interface. Each air cylinder is capable of generating 1,590 lbf at 100 psi, resulting in a total applied force of 3,180 lbf. These cylinders were chosen because of their ability to reach loads high enough to generate full pressure at the wheel / rail interface and for their bi-directional control so that the wheel could be retracted from the rail just as quickly as it was applied.

## 2.2. Components

---

### 2.2.5 Motor Control

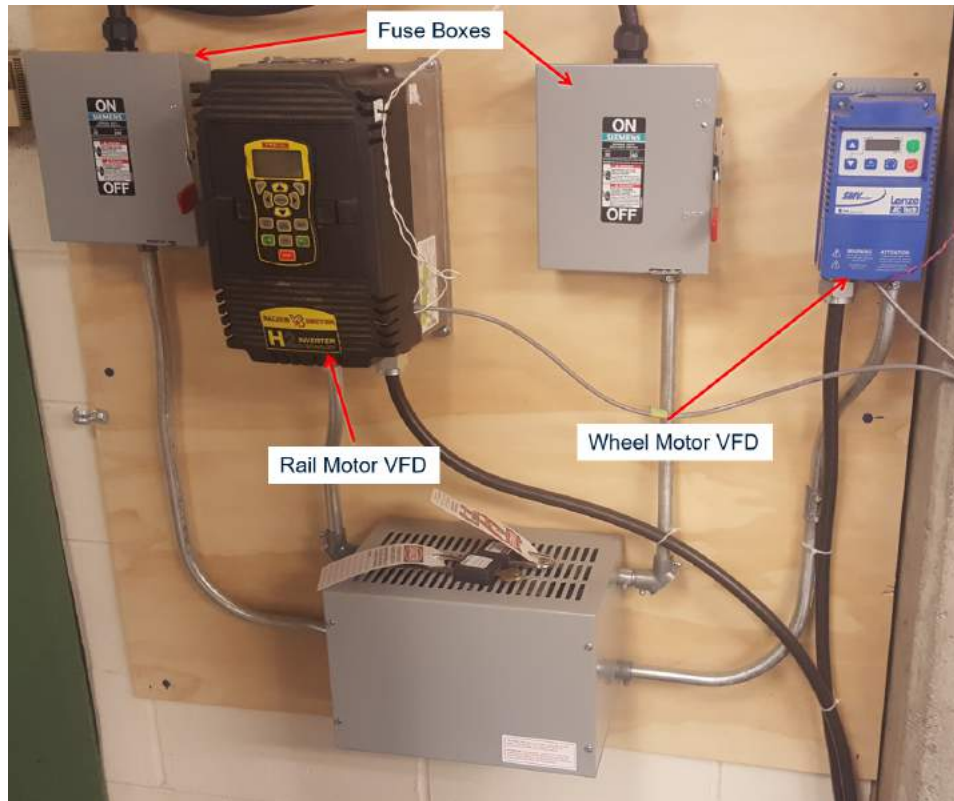


Figure 2.6: VFD's and supporting components to control the motor speeds.

Motor speed control on the machine is managed using variable frequency drives (VFD) which are shown in Figure 2.6 and described below. Two different VFD's were used because of cost and availability, but in the future I would recommend using two of the same type to make implementation simpler.

- **Fuse Boxes:** High voltage quick response fuses. Quick response fuses were selected for added safety.
- **Rail Motor VFD:** Baldor VS1SP AC V/Hz and sensorless vector control, 208 V, 3 phase variable frequency device.
- **Wheel Motor VFD:** Lenz SMV NEMA 1 (IP31), 5 hp, 208 V 3 phase variable frequency device.

### 2.2.6 DAQ Interface

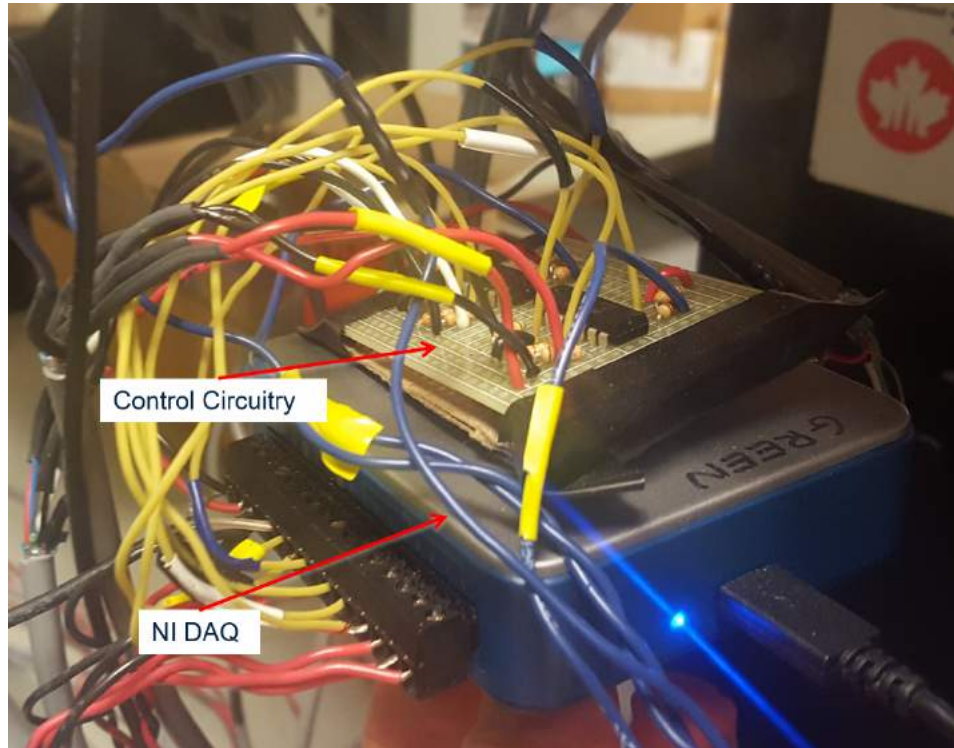


Figure 2.7: NI DAQ module and signal conditioning electronics.

The DAQ and supporting circuits used to interface the machine to the controller software is shown in Figure 2.7 and described below:

- **NI DAQ:** National Instruments USB-6001 Multifunction I/O device, 14-Bit resolution and 20 kS/s sampling rate. The DAQ is used to record all the sensors on the machine. The digital outputs on the DAQ are used for solenoid control and for controlling the speed of the motors via the VFD's.
- **Control Circuitry:** The VFD's accept digital signal control at a voltage of 10 V and 24 V, so additional circuitry is required to boost the DAQ digital out signals to levels sufficient for the two VFD's. See Appendix C for details.

### 2.2.7 Software Controller

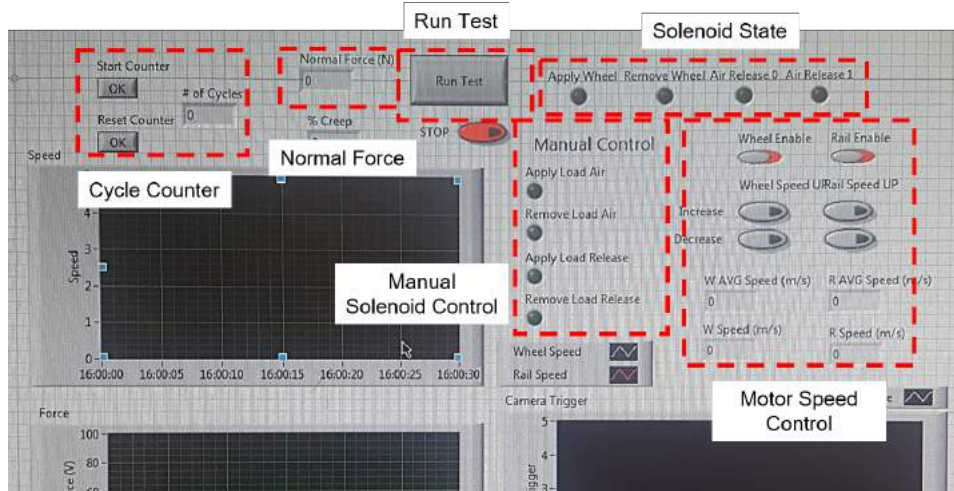


Figure 2.8: Software interface for the wheel/rail transfer machine.

The controller program, designed in LabVIEW, is used to set up experiments and control the operational parameters on the machine. It is shown in Figure 2.8 and described below:

- **Cycle Counter:** Keeps track of the number of complete cycles of the rail. 1 cycle = 4.454 m (the length of the band saw blade). Used for tracking long term carry-down experiments.
- **Normal Force:** The measured normal force applied at the wheel/rail interface as measured by the sensor shown in Figure 2.9.
- **Run Test:** This button runs the standard carry-down test. The motors need to be set to their desired speed before pressing this button. After pressing this button, the machine will engage wheel just before the initial product patch applying the desired pressure to the rail and then will retract the wheel from the rail after 7 wheel/rail interactions (the maximum amount of wheel and new rail interactions that the machine is capable of). The motors are then powered down and stopped.
- **Solenoid State:** Status LED's displaying which solenoid is active. The solenoids control the direction of air pressure (Figure 2.5).

## 2.2. Components

---

- **Manual Solenoid Control:** The solenoids can be controlled using these buttons when running experiments manually (without preset timing and control).
- **Motor Speed Control:** Speed control and output for the two motors. These controller buttons connect to the VFD's in Figure 2.6.

### 2.2.8 Measurement Sensors

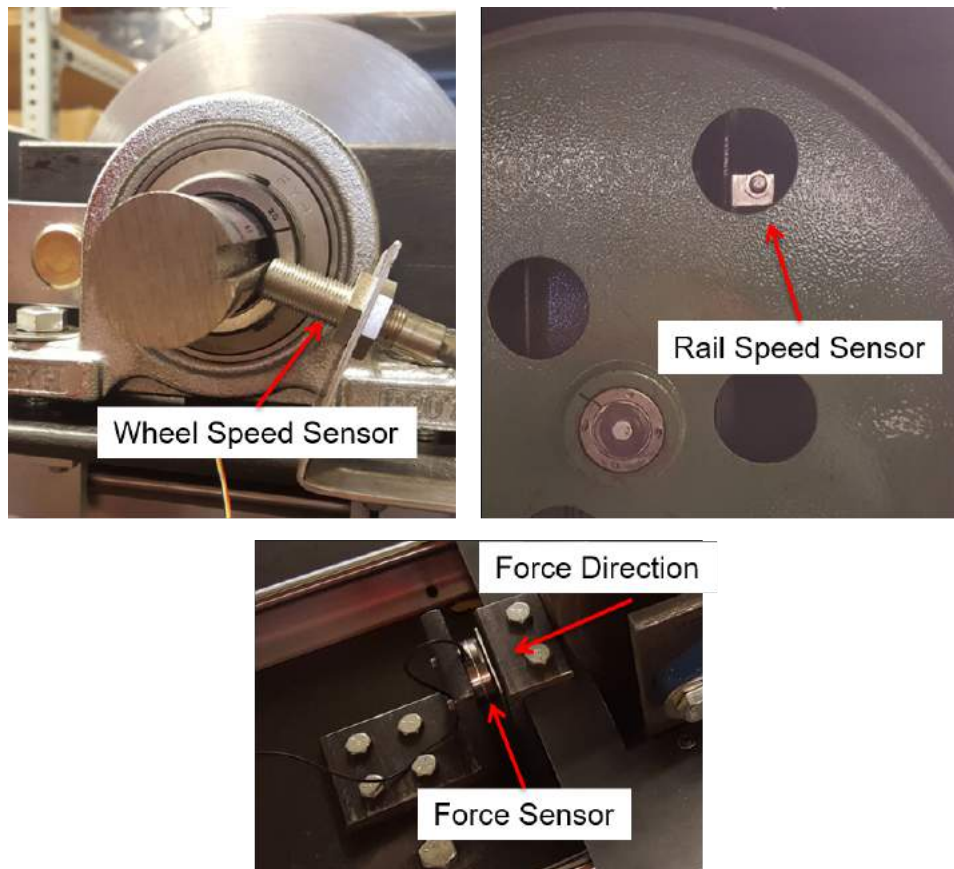


Figure 2.9: Locations and types of measurement sensors used on the machine.

The primary measurement sensors are shown in Figure 2.9 and described below:

- **Wheel and Rail Speed Sensor:** Magnetic Hall effect sensors with 15 kHz sampling frequency (66 ms) are used to measure the speed of the wheel and the rail. The sampling rate of these sensors is more than adequate for the speeds that the machine will be run at.
- **Force Sensor:** An FC2311 2000 lbf load cell force sensor (20 lbf/mV sensitivity with  $\sim 1$  mV noise) is placed behind the dummy wheel (see also Figure 2.3) measuring the applied load at the wheel/rail interface. A drawback is that this sensor only works for 2/3 of the applied pressure range (max applied pressure could be 3150 lbf). Despite this, this sensor was chosen because of its low cost (1/5 the price of the next range up) and its good resolution in the low range. The initially planned experiments would only operate in a pressure range within this sensor's capabilities. If future experiments require higher pressure, a new sensor can easily be swapped in. The load cell was powered with a 5 V supply.

## 2.3 Capabilities

The rail and the wheel are powered by two independent motors. The rail is powered by a 7.5 hp, 3490 rpm motor and the wheel is powered by a 5 hp, 1800 rpm motor. This allows for independent speed control of the rail and wheel allowing for experiments with small amount of creep to be performed. The theoretical top speed for an experiment is 18 m/s. 8 m/s is the maximum speed that an experiment has been currently conducted at.

Two tie rod air cylinders operating at a pressure of 100 psi each produce 3180 lbf. In this set up, 3150 lbf (14 kN) over a 10 mm line using a Hertzian contact patch would result in 1033 MPa of pressure at the contact surface representative of a common fully loaded freight train.

The rail surface is 4.454 m long and the wheel has a circumference of 0.578 m. This allows for 7 complete wheel/rail interactions where the wheel interacts with a new piece of rail.

Table 2.1 summarizes the machines capabilities.

### 2.3. Capabilities

---

Component	Details
Speed range	0 m/s to 18 m/s <sup>1</sup>
Independent wheel/rail speed control?	Yes <sup>2</sup>
Force range	0 kN to 14 kN <sup>3</sup>
Number of wheel/rail interactions	7 <sup>4</sup>

Table 2.1: Machine capabilities.

---

<sup>1</sup>Theoretical maximum speed. The highest speed that has currently been tested is 8 m/s.

<sup>2</sup>Allows for the testing of creep.

<sup>3</sup>Capable of a higher force if a greater initial air pressure source is used.

<sup>4</sup>7 is the maximum number of wheel interactions with a previously untouched section of rail. After this the wheel will be interacting with sections of the rail that have already been rolled on.

# Chapter 3

## Methods

### 3.1 Application of KELTRACK®

The KELTRACK® product is analogous to a house hold paint when it is wet in terms of texture and appearance. When it dries, it feels like a waxy paint substance to the touch.

For the majority of experiments KELTRACK® is initially applied to the rail before the wheel passes through, initiating the carry-down experiment. Even though the early experiments to be conducted with this machine were primarily qualitative, a reasonably consistent starting volume of KELTRACK® was desired to minimize variability in experimental results outside of the controlled change in parameters.

The thickness of KELTRACK® to be initially applied was determined by finding the thickest amount of product that could be deposited while maintaining a consistent thickness throughout the product coverage. Because the rail is orientated vertically, the product would inevitably drip down resulting in some variance in thickness. A final value of 0.5 mm was determined through trial and error.

Two metal shims, each 0.5 mm thick, were attached to the rail using a magnet placed behind to hold them tightly in place. KELTRACK® was liberally applied and then the excess was scraped off the top with a razor blade leaving a consistent height across the area of interest. The final dimensions were 50 mm long x 0.5 mm thick. The width of the product interaction is determined by the width of the wheel, which is 10 mm. The process and final result is shown in Figure 3.1. There was still some slight dripping of product due to the weight, but it was consistently seen between applications and deemed acceptable for these early experiments.

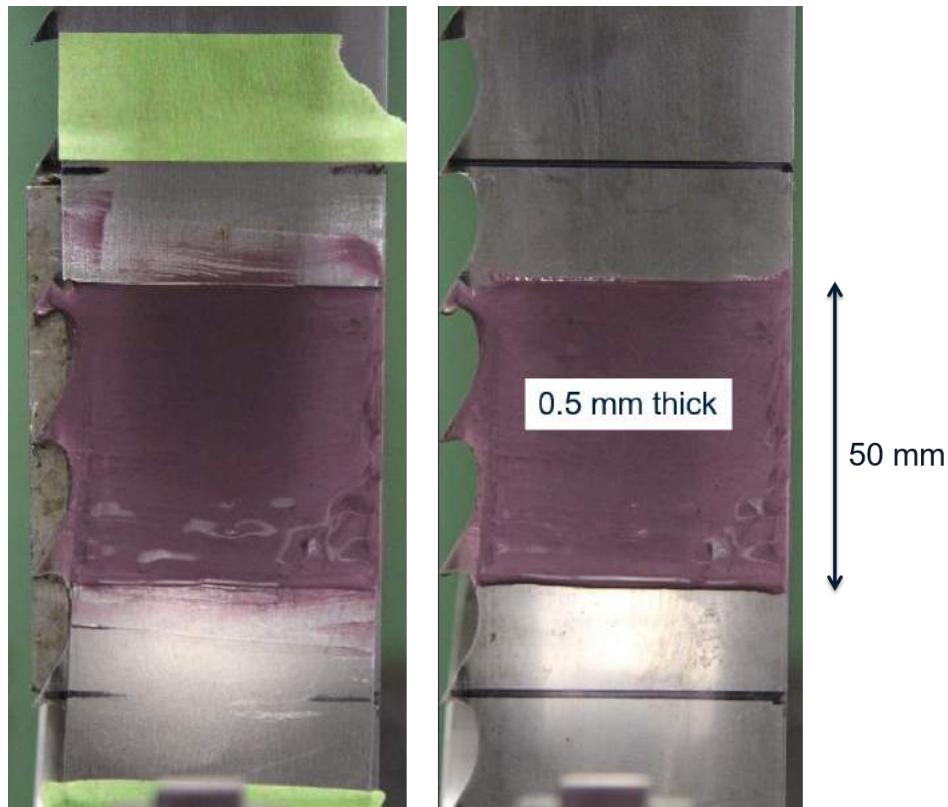


Figure 3.1: Application method for the initial patch of KELTRACK®.

### 3.2 Fluorescent Additive

Previous research showed that there were frictional benefits on rail that had been exposed to a liquid friction modifier even when the product appeared to have worn off because it could not be seen visually under ambient light with the naked eye. This led to the exploration of other visualization techniques for the purpose of observing the carry-down behaviour of KELTRACK®. Rhodamine-B was selected as the fluorescent dye to be mixed in with KELTRACK® and was added at a concentration of 0.03 % by weight. A side effect of using Rhodamine-B is that it turns KELTRACK® from grey to purple.

Rhodamine-B has a peak excitation wavelength of 554 nm and a peak emission wavelength of 579 nm (Figure 3.2). A 532 nm green laser was used to excite the KELTRACK®-Rhodamine-B solution with a filter on

### 3.2. Fluorescent Additive

the camera to isolate the emission spectra (Figure 3.3).

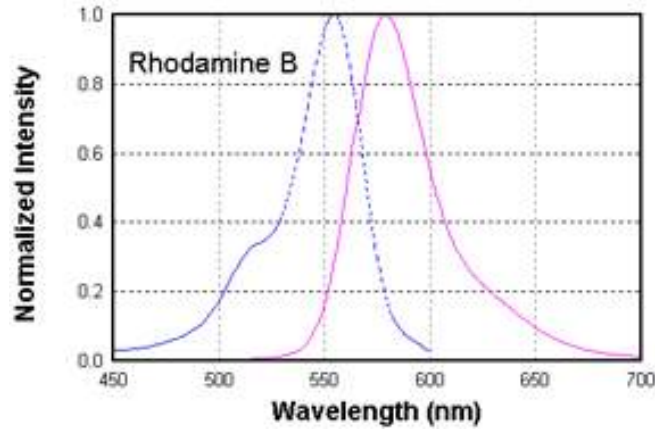


Figure 3.2: Rhodamine-B excitation (dashed blue line) and emission (solid pink line) spectra [21].

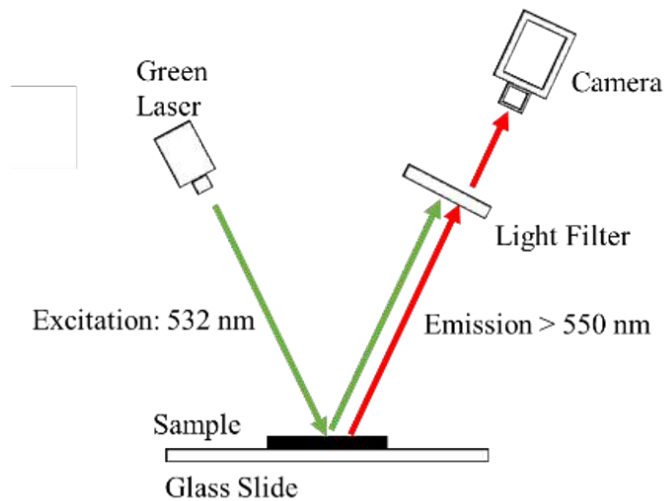


Figure 3.3: Rhodamine-B detection schematic [14].

Hatef Rahmani [14] ran shear stress and shear viscosity tests comparing original KELTRACK® with KELTRACK® that had Rhodamine-B added. The results seen in Figure 3.4 show no noticeable effect on these properties of KELTRACK® from the addition of Rhodamine-B.

### 3.2. Fluorescent Additive

---

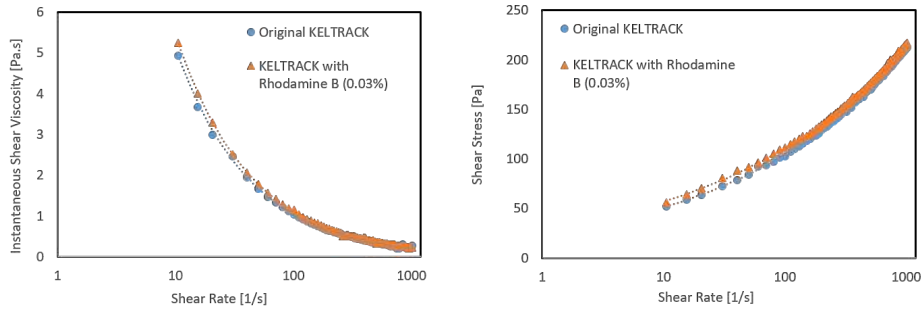


Figure 3.4: Shear stress and shear viscosity comparison of KELTRACK® with and without Rhodamine-B [14].

Figure 3.5 shows that by adding Rhodamine-B to KELTRACK® it becomes easier to visualize the presence of KELTRACK® providing a valuable benefit for observing and understanding product carry-down.

It should be noted that the laser used is highly localized with a very narrow viewing angle which may give the appearance of less product in the surrounding area than is actually true.

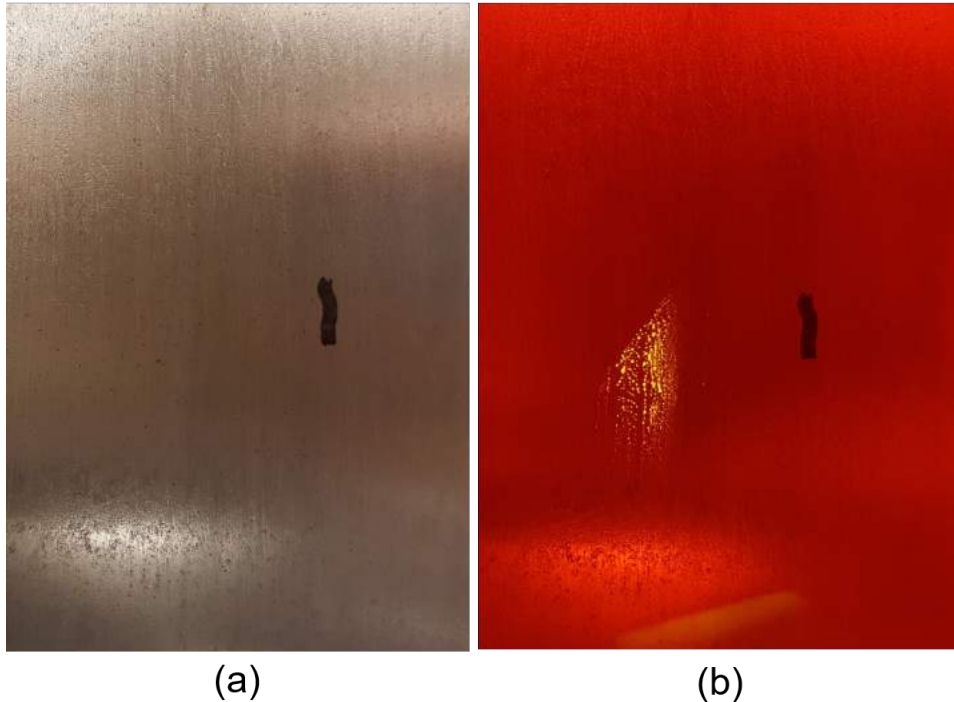


Figure 3.5: Same section of rail showed in (a) ambient light and with (b) fluorescence showing the benefit of fluorescence as a visual aid. The light spots near the top and bottom of the images are reflections from the ambient light.

### 3.3 Control of Speed and Pressure

The motors used to drive the rail and wheel are both connected to VFD's (Figure 2.6). Each motor is run on 60 Hz power and each motor is capable of changing the frequency (speed) in 0.1 Hz increments. The VFD's are controlled by the software controller (Figure 2.8). However, due to the implementation of the software controller and DAQ interface electronics (Figure 2.7) the increment/decrement step size is limited to 0.3 to 0.4 Hz (the full speed range is 0 Hz to 60 Hz) . The actual speed of the rail and wheel are measured by the speed sensors attached to the machine (Figure 2.9). Because of the slight variability in step size for each VFD, exact speed matching for the wheel and rail is often quite difficult. The difference can be as great as 0.05 m/s.

When running an experiment the motor speed is incrementally controlled by the software controller until the desired speeds (as read by the speed sensors) are achieved. At this point the motors are paused so that the product can be applied to the rail, the motors are then resumed, quickly ramping up to their previously set speed so that the experiment can be run. This method minimizes the potential drying of the product before wheel/rail interaction.

The pressure is controlled using a manual pressure regulator (Figure 2.5). The pressure is the first thing that is set when running an experiment and is done before the motors are turned on. It has no effect on the machine operation until the air cylinders are activated by the software controller.

## 3.4 Experimental Operation

The machine is set up such that once the pressure is set, the motor speeds have been set and paused, and the product is applied to the rail there are only two steps remaining for running an experiment: 1) The motors are resumed and allowed to ramp back up to the desired speed. 2) Once the desired speed is reached the operator presses “Run Test” (Figure 2.8) to run the experiment. A photo diode sensor (Figure 3.6) reading a marker on the rail triggers the air cylinders to engage the wheel onto the rail resulting in 7 wheel/rail interactions after the product pickup by the wheel from the initial application patch before finally disengaging the wheel from the rail and stopping the motors bringing the experiment to a finish. The same trigger sensor is also used to control a high speed camera which can be optionally attached to record the transfer of product at the wheel/rail interface.

In between the experiments, the product is cleaned off of the wheel and rail using a multi-stage process. KELTRACK® is water soluble, so the product is initially washed off with a wet rag. This removes most of the product. The product is then completely removed using 1000 grit and 2000 grit sandpaper so a clean smooth surface remains. This was the method recommended by L.B. Foster who manufactures the KELTRACK® product.

### 3.4. Experimental Operation

---

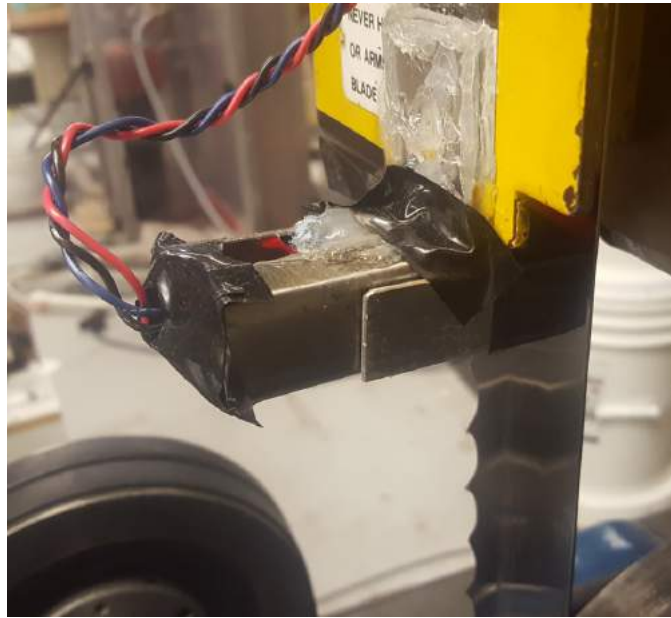


Figure 3.6: A photo diode sensor used for triggering events.

## Chapter 4

# Experiments & Results

### 4.1 Initial LFM Carry-down Experiments

The purpose of this experiment was to conduct initial baseline product carry-down tests. Experiments were conducted at a pressure of 25 psi ( $\sim 1/4$  full train pressure) and a wheel/rail speed of 1 m/s ( $\sim 1/15$  full speed). KELTRACK® was applied to the rail, the wheel would then pick up the KELTRACK® under pressure and at speed and then 7 wheel/rail interactions with a clean rail surface each time would occur before the experiment ended.

The initial KELTRACK® application on the rail is shown in Figure 3.1. Some slight pooling due to gravity because the rail is orientated vertically can be seen near the bottom of the initial patch. This effect was minimized by using a thin (0.5 mm) initial patch. The initial distribution patch was consistent between experiments providing confidence at the potential for repeatability in the volume of the initial KELTRACK® patch under the wheel/rail contact path. Figure 4.1 shows the initial KELTRACK® application patch after the wheel has rolled through. In all these photos the rail is moving from top to bottom with respect to the page orientation. Several key observations about this figure can be made:

1. Under ambient light KELTRACK® is not visible down the centre high pressure contact patch, but using fluorescence you can indeed see traces of KELTRACK® in this region supporting the benefit of adding Rhodamine-B to the product for aiding in visualization.
2. The KELTRACK® that can be seen down the centre patch has distinct lines that appear to match accordingly with small scratches seen on the surface of the wheel (Figure 4.2). The scratches on the wheel are roughly 100  $\mu\text{m}$  wide. The depth is unknown.
3. The edges of KELTRACK® nearest where the wheel rolled through are thicker than the initial application, indicating that the product was

#### 4.1. Initial LFM Carry-down Experiments

---

squeezed out from the wheel/rail contact patch laterally out towards the sides.

4. There is a trail of KELTRACK® extending forward from the initial application patch indicating that the product is also pushed forward longitudinally under the low pressure edges as the wheel rolls through the initial application patch.

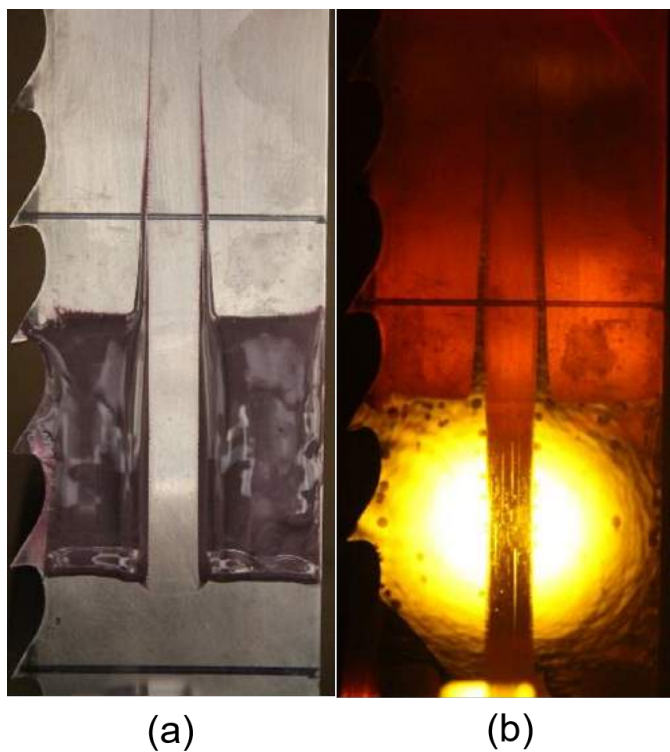


Figure 4.1: Initial carry-down experiment, interaction #0: (a) Ambient light. (b) Fluorescence. Because of the narrow field of the laser used, only a small section is illuminated and can be saturated.

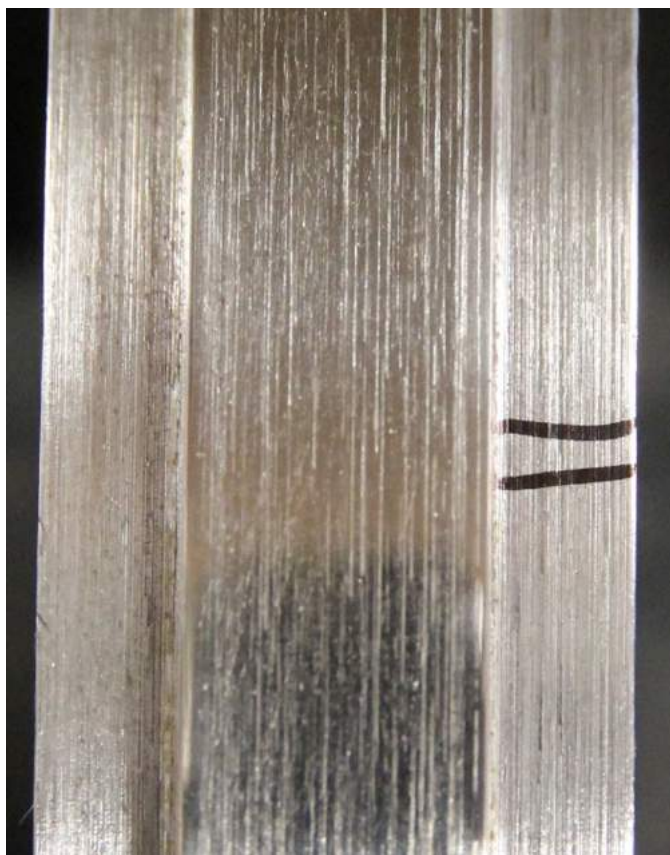


Figure 4.2: Zoomed in section of a clean wheel showing minor scratches on the surface. The scratches are roughly  $100\ \mu\text{m}$  wide on average.

Figure 4.3 shows the results from interaction #1 and interaction #3. There are distinct lines of KELTRACK® from the edges of the wheel/rail interface without any visible product down the centre. Upon closer inspection it was believed that the wheel was slightly crowned leading to full pressure only being developed down the centre patch of the wheel/rail interface. Along the edges of the wheel full pressure is not developed so instead of KELTRACK® being squeezed out, it is picked up by the wheel along the top surface edges and able to be carried down. The KELTRACK® is squeezed out from the high pressure centre patch and thus is not picked up by the wheel and not carried down for further wheel/rail interactions. Additionally it appears that less product is transferred from wheel to rail in interaction #3 than was transferred in interaction #1.

#### 4.1. Initial LFM Carry-down Experiments

---

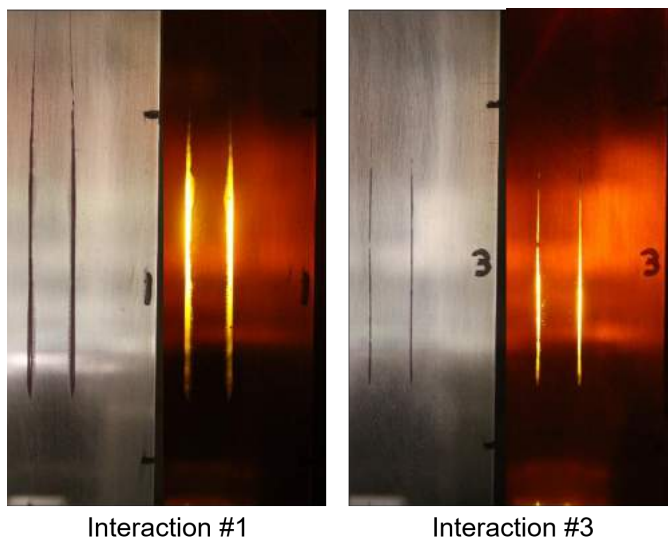


Figure 4.3: Interaction #1 & #3.

Figure 4.4 shows the results from interaction #5 and what is left on the wheel after the experiment is complete. At interaction #5 there is very little product that has been transferred from the wheel to the rail. Interactions #6 and #7 are not shown because no product transfer was observed on the rail for either of these interaction locations. The wheel shows a concentration of product along the edges as is expected from the crowning and what was seen with the transfer on the rail. There is also some product seen down the centre patch in distinct short straight lines. It is believed that there are micro scratches in the surface of the wheel and product has been squeezed into these scratches which behave as low pressure regions similar to the crowned edges of the wheel. The product stays in these cracks throughout the experiment and does not transfer to the rail during operation.

#### 4.1. Initial LFM Carry-down Experiments

---

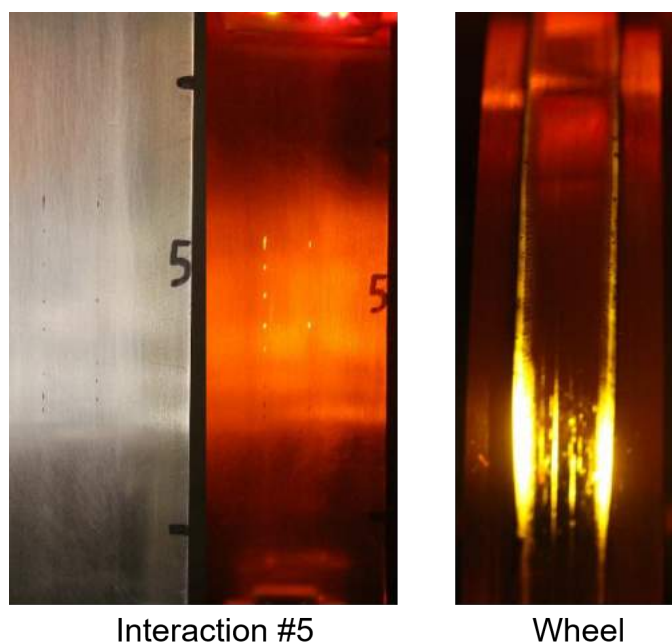


Figure 4.4: Interaction #5 & the wheel after the experiment is complete. Again, saturation can be seen under fluorescence

Following these initial results Fujifilm Prescale HHS PS pressure paper was used to better visualize the crowning of the wheel. The pressure sensitive paper is placed between the wheel and rail under a pressure of 25 psi. The result is shown in Figure 4.5. In this example full pressure was only achieved over a 9.7 mm centre width (the wheel width is 10 mm). The crowning was not perfectly uniform along the circumference of the wheel. At points along the wheel surface the width of the wheel surface where full contact pressure was achieved was as low as a 8.2mm. This pressure paper test confirms what was seen in the experiments that the surface of the wheel was no longer trued parallel with the rotation axis and thus there are high pressure and low pressure zones in the wheel/rail contact area leading to the way with which we saw KELTRACK® was transferred from the rail to the wheel initially.

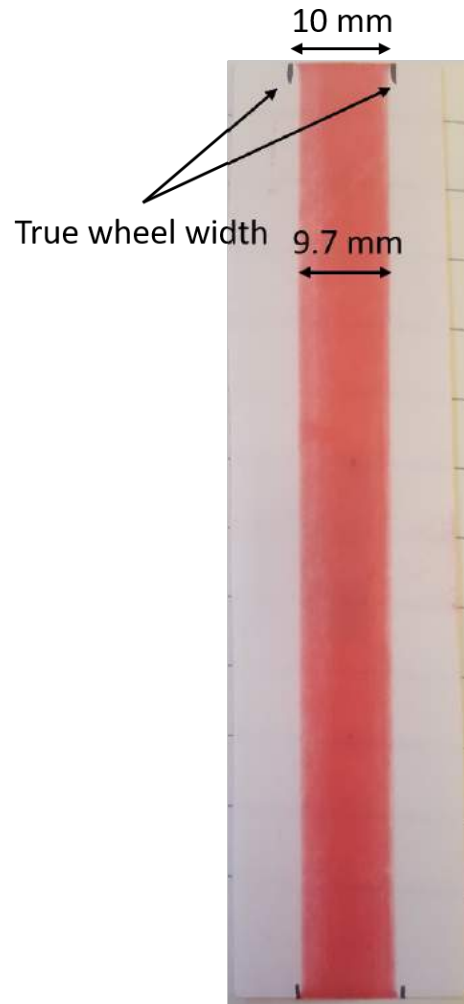


Figure 4.5: Pressure profile of the wheel/rail interaction for a section of the wheel. Fujifilm Prescale HHS PS pressure paper was used. The paper is initially completely white and turns red under applied pressure.

A high speed camera was also used in this experiment recording the initial product transfer from the rail to the wheel at interaction #0. Figure 4.6 shows several screen shots of the process clearly displaying film splitting and the formation of filaments as was expected [5].

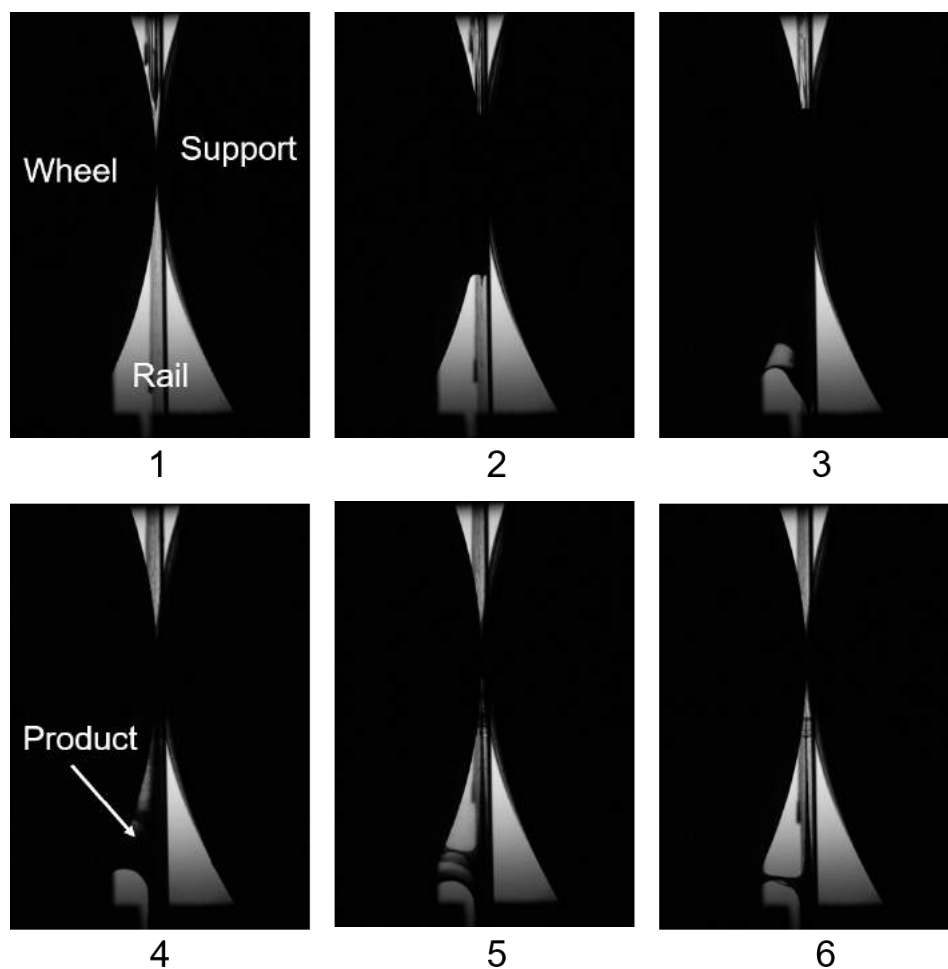


Figure 4.6: Snapshots captured by the high speed camera showing the film splitting action as the product is initially transferred from the rail to the wheel. Time is increasing from 1 to 6. The rail is moving from top to bottom.

In conclusion the wheel was able to pick up product from the rail and replicate 7 wheel/rail interactions displaying carry-down behaviour. Very little or no KELTRACK® was picked up by the centre patch of the wheel and transferred back to the rail on subsequent wheel/rail interactions. In contrast, a noticeable amount of KELTRACK® was picked up by the wheel along the edges and transfer from the wheel to rail was seen up to and including interaction #5 along these edges. This is likely due to the slight

crowning of the wheel leading to full pressure only being developed down the centre path which squeezes the product out during interaction #0. It is only the low pressure zones (specifically the wheel edges) where the product is picked up by the wheel. There was no product observed on the rail after interactions #6 and #7, but there was still product visible on the wheel in the low pressure zones after the 7 wheel/rail interactions and the completion of the experiment.

## 4.2 Long Term LFM Carry-down Experiment

The purpose was to explore the long term carry-down behaviour of dry KELTRACK®. Previous experiments had only explored 1 to 7 wheel/rail interactions simulating a maximum of 4.454 m of product carry-down on the wheel/rail transfer machine. This experiment was designed to simulate 9,030 wheel/rail interactions for a total simulated track distance of 5,745 m on the wheel/rail transfer machine.

KELTRACK® was thinly applied to a 90mm long section along the wheel. The amount of product was not tightly controlled, but full and roughly uniform coverage was the desired goal. The product was allowed to air dry at room temperature for 30 min. This was the amount of time it took for the product to be dry to touch such that the product did not transfer as a wet felt film under light pressure from a finger. The reasoning behind this was to represent the working theory that KELTRACK® would be picked up by the wheel at low contact pressure zones and would dry on the wheel before experiencing full contact pressure in these locations as the train wheel enters a curved rail section (Figure 5.1). Figure 4.7 shows the initial KELTRACK® application on the wheel after it has dried. The operational conditions for this experiment are shown in Table 4.1, the wheel and rail were set at the same speed.

Speed (m/s)	1.9
Pressure (psi)	25

Table 4.1: Speed and pressure conditions for the long term product carry-down experiment.

For this experiment the machine was paused at various intervals so that photos and observations could be recorded. The rail and wheel were cleaned at each of these intervals (excluding the initial application location). The reason behind this was to have the wheel interact with a simulated fresh

#### 4.2. Long Term LFM Carry-down Experiment

---

patch of rail as much as possible. The ideal scenario would be to clean the rail after each complete revolution of the length of rail (4.454 m) as this would ensure the KELTRACK® on the wheel is always interacting with a completely clean and new piece of rail. The time investment behind this operation is considerable and would make it difficult to achieve a long distance in a reasonable amount of time. For this initial long term carry-down experiment an assumption was made that only cleaning the rail at certain stages would still provide information that was satisfactory for this early qualitative stage. Table 4.2 shows the stages during the experiment that the machine was paused and observations were made along with wheel/rail cleaning if necessary.

# of Wheel/Rail Interactions	Distance (m)	Cleaned (y/n)
0	0	y
287	182	y
1,715	1,091	y
3,486	2,218	n
5,236	3,331	n
9,030	5,745	n

Table 4.2: The stages when the machine was paused so that observations could be made and cleaning if necessary. Cleaning of the wheel and rail was not needed after 3,486 interactions as no KELTRACK® was observed on the rail or wheel (except the initial application location).

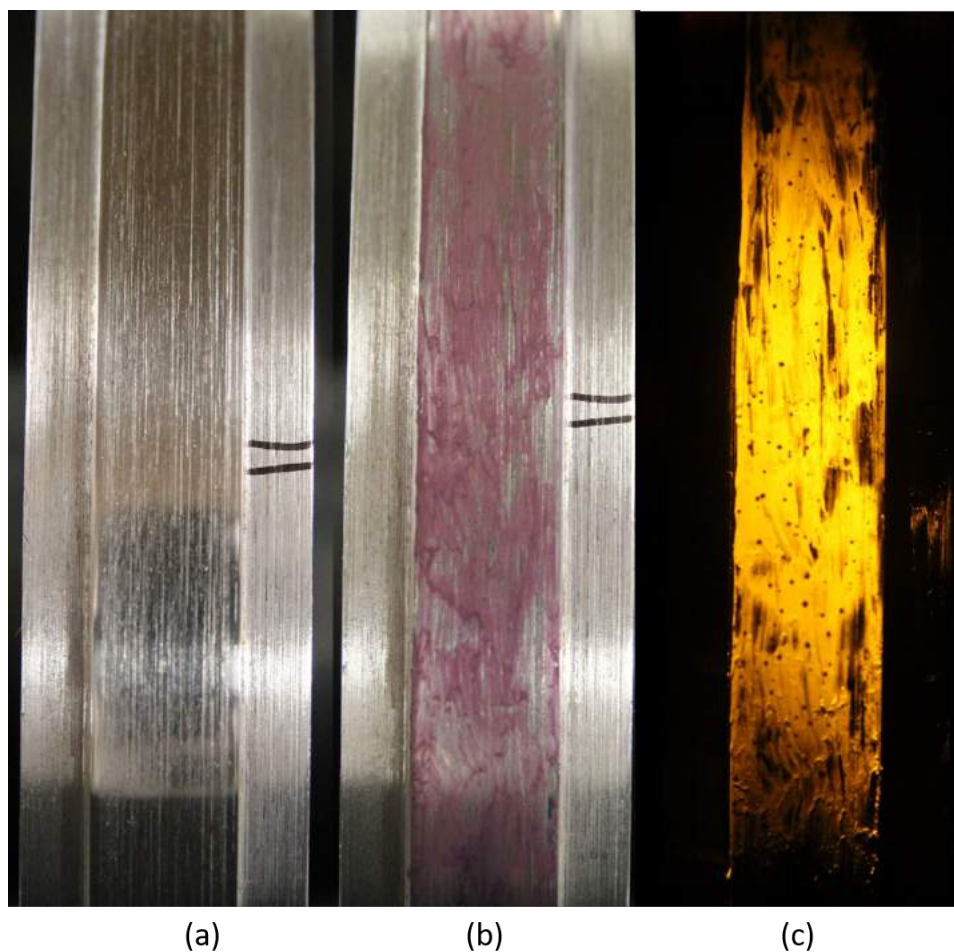


Figure 4.7: (a) Cleaned section of the wheel. (b) Initial application of dried KELTRACK® viewed in ambient light. (c) Viewed using Fluorescence.

Figure 4.8 shows the KELTRACK® coverage on the wheel after various stages. 0 m represents the initial KELTRACK® patch before the experiment is run. Looking at the 0 m, 182 m and 1,091 m photos the KELTRACK® product appears to wear off more rapidly in the early stages of carry-down. Compare this with the photos for 2,218 m, 3,331 m and 5,745 m where the rate of product wear appears to have decreased. This result is reasonable as we would expect to see a higher rate of KELTRACK® wear on the wheel early on during carry-down when there is more product present in high pressure zones. The product wear rate would then decrease

#### 4.2. Long Term LFM Carry-down Experiment

---

as KELTRACK® mostly remains in low pressure zones later on in the carry-down process. Figure 4.9 shows this phenomena as KELTRACK® mostly appears in concentration along the low pressure edges of the wheel and down the middle in surface scratches on the wheel.

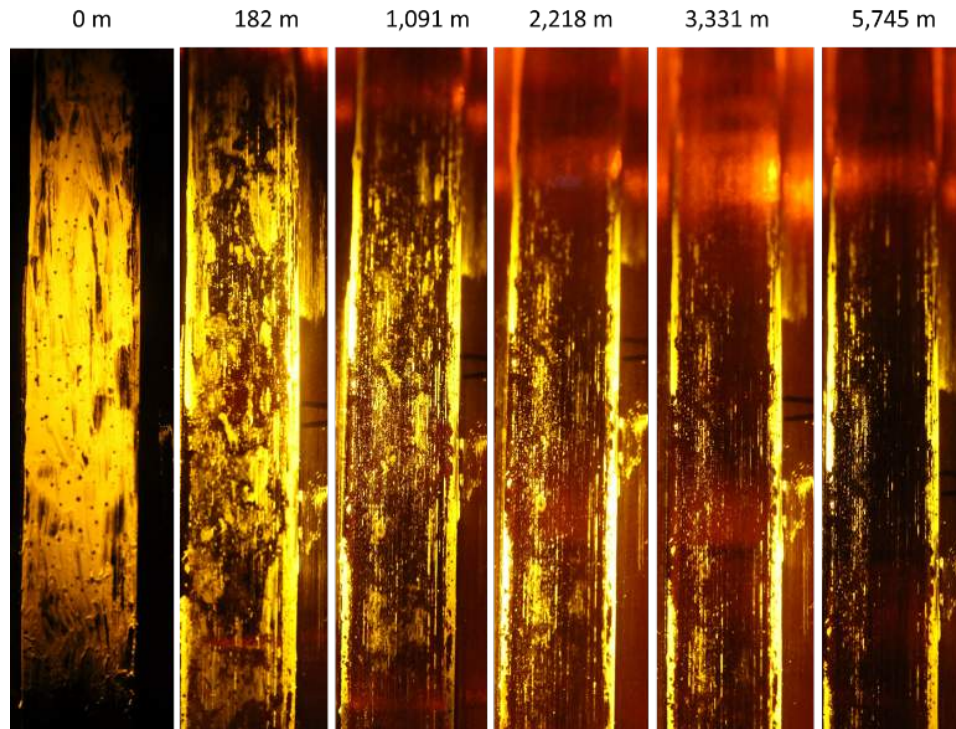


Figure 4.8: Comparison at each of the observation stages of the KELTRACK® coverage on the wheel, viewed using fluorescence.

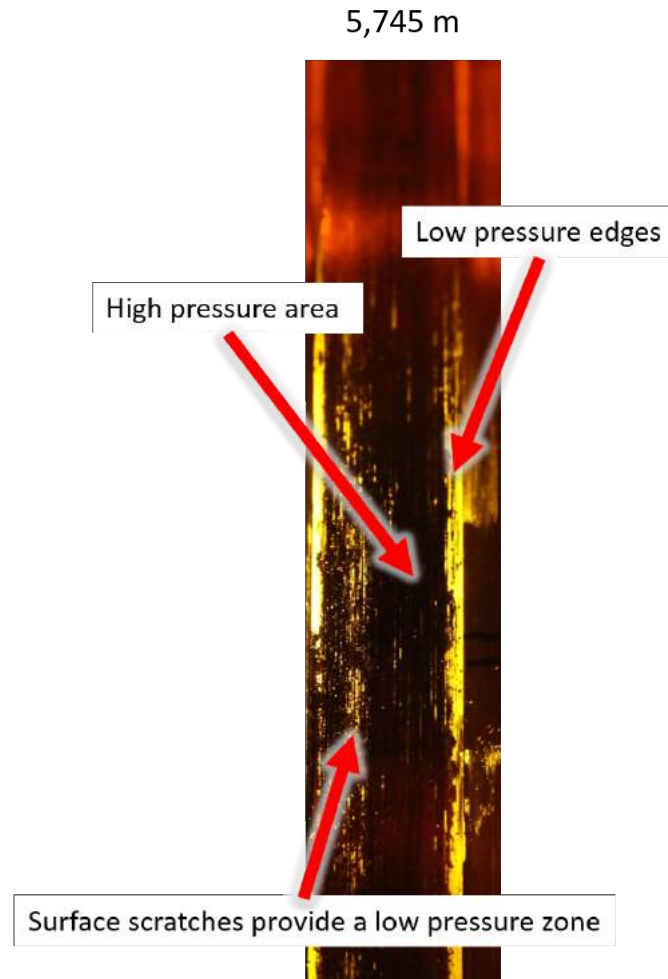


Figure 4.9: The wheel after the 5,745 m stage showing the remaining KELTRACK® coverage in the high and low pressure zones.

After 287 wheel/rail interactions (182 m) the experiment was paused for inspection of the wheel and rail. In addition to the expected wear of the initial KELTRACK® patch on the wheel two other interesting phenomena were observed: 1) KELTRACK® was transferred from the wheel to the rail. This can be seen in Figure 4.10. The transfer of wet KELTRACK® from wheel to the rail was observed previously and was expected, but the transfer of dried KELTRACK® from wheel to rail had not been experimentally observed before. 2) KELTRACK® could be seen on the wheel at secondary

#### 4.2. Long Term LFM Carry-down Experiment

---

locations, different from the initial application location indicating that after the wheel was transferring KELTRACK® to the rail, there was then further transfer from the rail to the wheel. In the field this could represent wheels further down the train picking up KELTRACK® that had been transferred from the wheels at the front of the train to rail. This rail to wheel transfer can be seen in Figure 4.11.

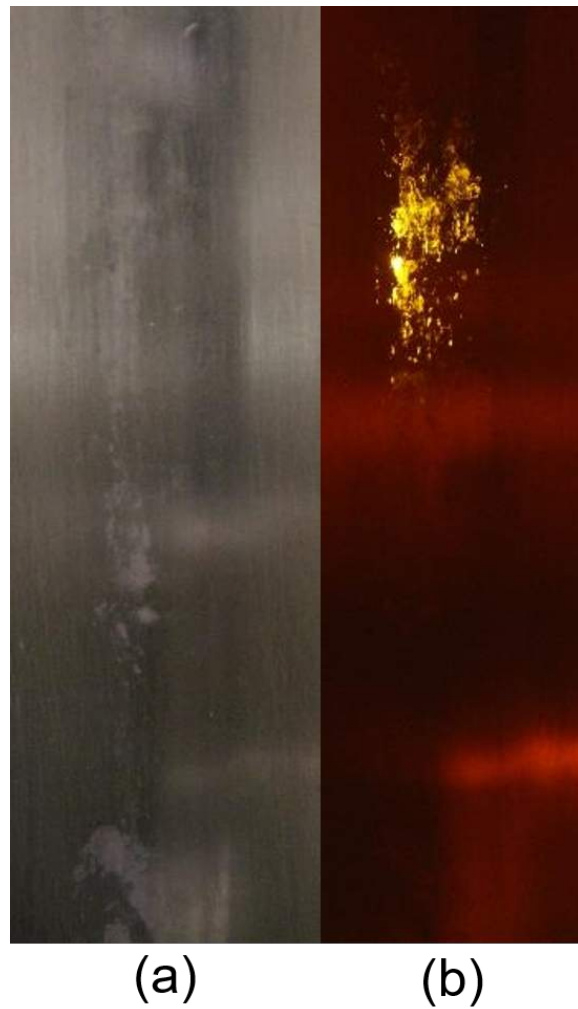


Figure 4.10: KELTRACK® transferred from wheel to rail after 182 m. (a) Ambient light. (b) Fluorescence.

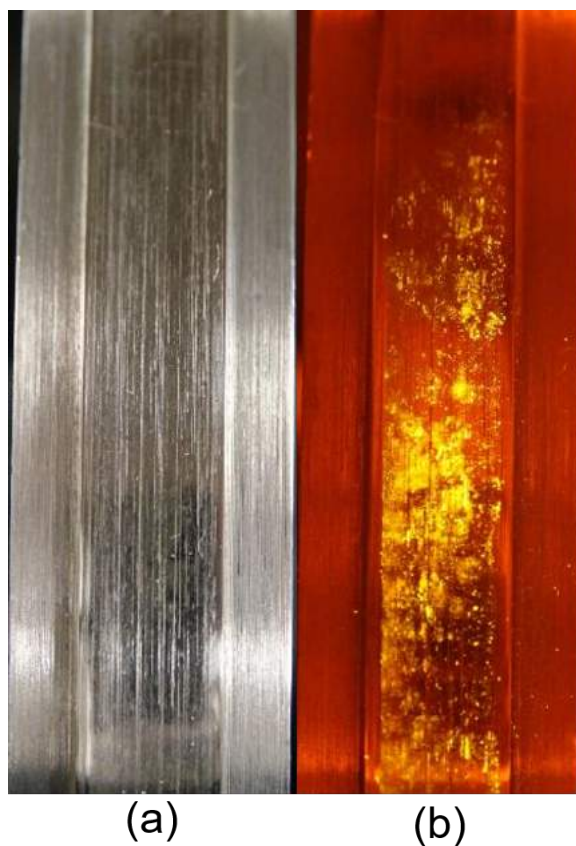


Figure 4.11: KELTRACK® previously transferred from wheel to rail now being picked up by the wheel after 182 m. (a) Ambient light. (b) Fluorescence.

After 287 wheel/rail interactions (182 m) the wheel and rail were cleaned removing all traces of KELTRACK®, except for the original application location which was left untouched. The experiment was continued and then paused after 1,715 wheel/rail interactions (1,091 m) for observation. As was seen in the previous stage KELTRACK® was again being transferred from the wheel to the rail and this transferred KELTRACK® was then being picked up by the wheel at secondary locations, different from the initial application site (Figure 4.12 & Figure 4.13). At this point the rail and wheel were again cleaned removing all traces of KELTRACK® (except at the initial application location). At the remaining observation stages (3,486 m, 5,236 m, 9,030 m) no further KELTRACK® was observed to

#### 4.2. Long Term LFM Carry-down Experiment

---

have transferred from the wheel to the rail.



Figure 4.12: KELTRACK® transferred from wheel to rail after 1,091 m. (a) Ambient light. (b) Fluorescence.

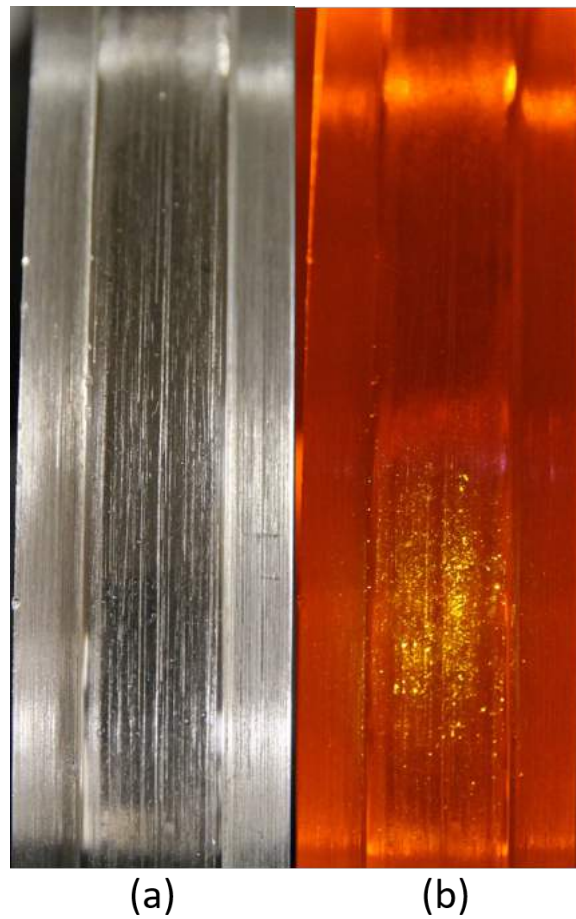


Figure 4.13: KELTRACK® previously transferred from wheel to rail now being picked up by the wheel after 1,091 m. (a) Ambient light. (b) Fluorescence.

In conclusion, a long term carry-down experiment of KELTRACK® with 9,030 wheel/rail interactions demonstrated dry film transfer and simulated significantly more wheel/rail interactions than previously conducted [16]. The wear behaviour of KELTRACK® was observed and recorded at six stages throughout the experiment.

### 4.3 Effect of Speed on LFM Carry-down

The purpose of this experiment was to explore the effect of speed on the carry-down behaviour of KELTRACK®. Previous experiments run at a manual feed, at 1 m/s, and at 2 m/s produced no observable difference, but an experiment at 4 m/s showed a slight increase in the carry-down of KELTRACK®. This difference was the motivation for the following experiment. For this experiment two different speeds were selected: 1) Manual feed and 2) 8 m/s. The wheel and the rail were set to the same speed and the pressure was set to 25 psi each time. KELTRACK® was initially applied to the rail on a 50 mm long patch with a uniform height of 0.5 mm. Three tests were conducted at each speed to provide a small repeatability comparison. Qualitatively the repeat experiments produced similar enough results to give confidence in the experiment. Figure 4.14 and 4.15 show examples of the repeats for the manual speed test at interaction #1. Figure 4.16 and 4.17 show examples of the repeats for the 8 m/s speed test at interaction #1. The remaining interactions for each speed were also compared and showed similar qualitative repeatability but are not shown here. Each test involved six unique wheel/rail interactions. The operational conditions are shown in Table 4.3. In all the images for this experiment the rail is moving from top to bottom with respect to the page.

Speed 1 (m/s)	Manual feed
Speed 2 (m/s)	8
Pressure (psi)	25

Table 4.3: Speed and pressure conditions for the effect of speed on carry-down experiment.

#### 4.3. Effect of Speed on LFM Carry-down

---

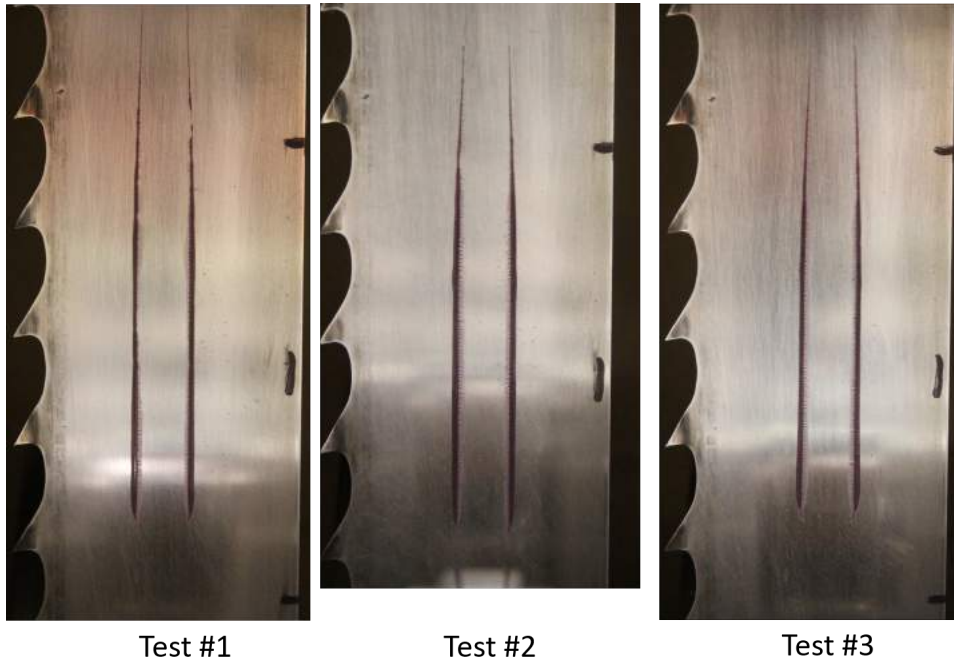


Figure 4.14: The results under ambient light at interaction #1 for each test at the manually fed speed showing good experimental repeatability.

4.3. *Effect of Speed on LFM Carry-down*

---

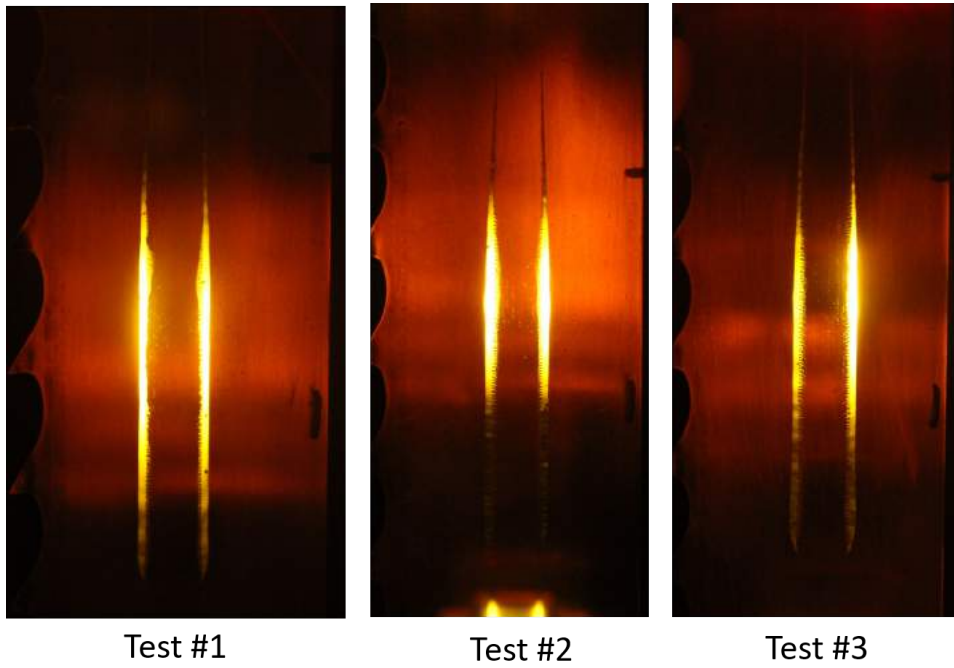


Figure 4.15: The results viewed with fluorescence at interaction #1 for each test at the manually fed speed showing good experimental repeatability.

4.3. *Effect of Speed on LFM Carry-down*

---

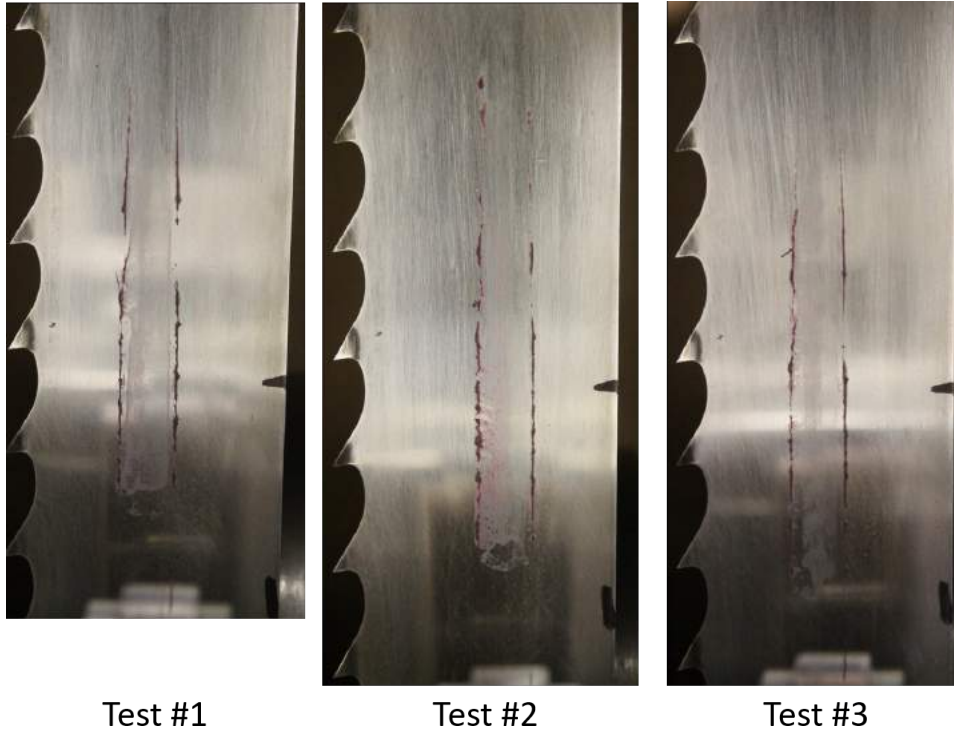


Figure 4.16: The results under ambient light at interaction #1 for each test at 8 m/s showing good experimental repeatability.

### 4.3. Effect of Speed on LFM Carry-down

---

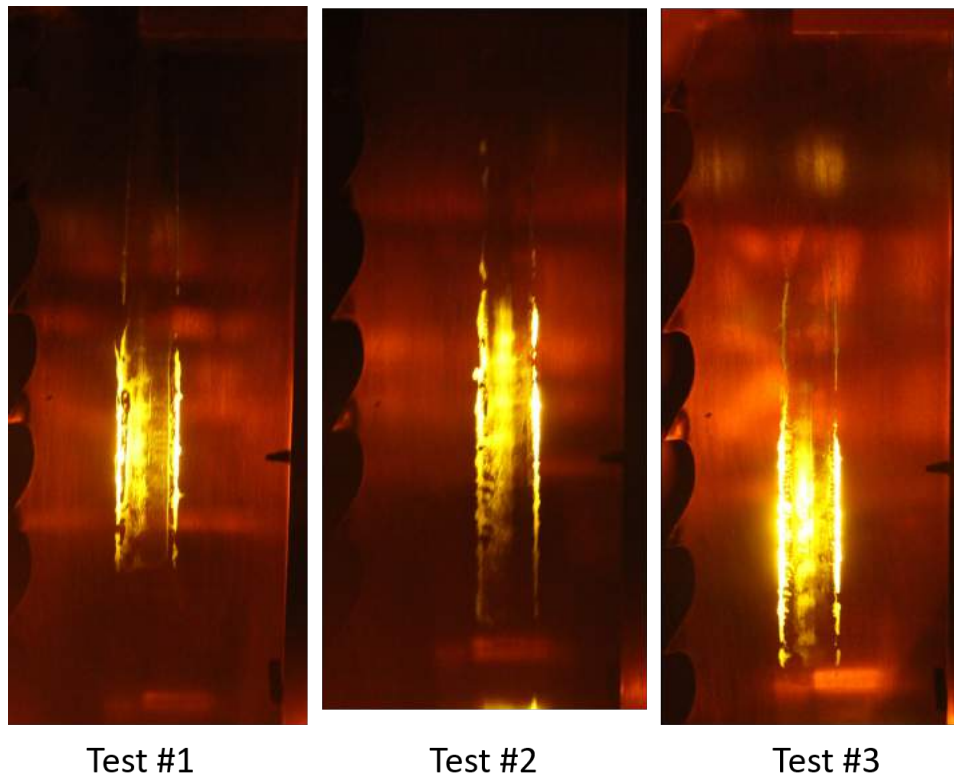


Figure 4.17: The results viewed with fluorescence at interaction #1 for each test at 8 m/s showing good experimental repeatability.

The results for the manually fed speed tests agreed closely with previous experiments under the same conditions. Looking at Figure 4.18 there is no observed KELTRACK® down the middle of the contact patch and the edges of the contact patch are quite clean and straight. By comparison, in the 8 m/s test KELTRACK® is observed down the middle of the contact patch and the edges of the contact patch are quite jagged and non-linear. In addition KELTRACK® from the initial application patch is pushed further down the rail than what was seen in the manually fed tests. Figure 4.19 shows the initial interaction location viewed in fluorescence.

### 4.3. Effect of Speed on LFM Carry-down

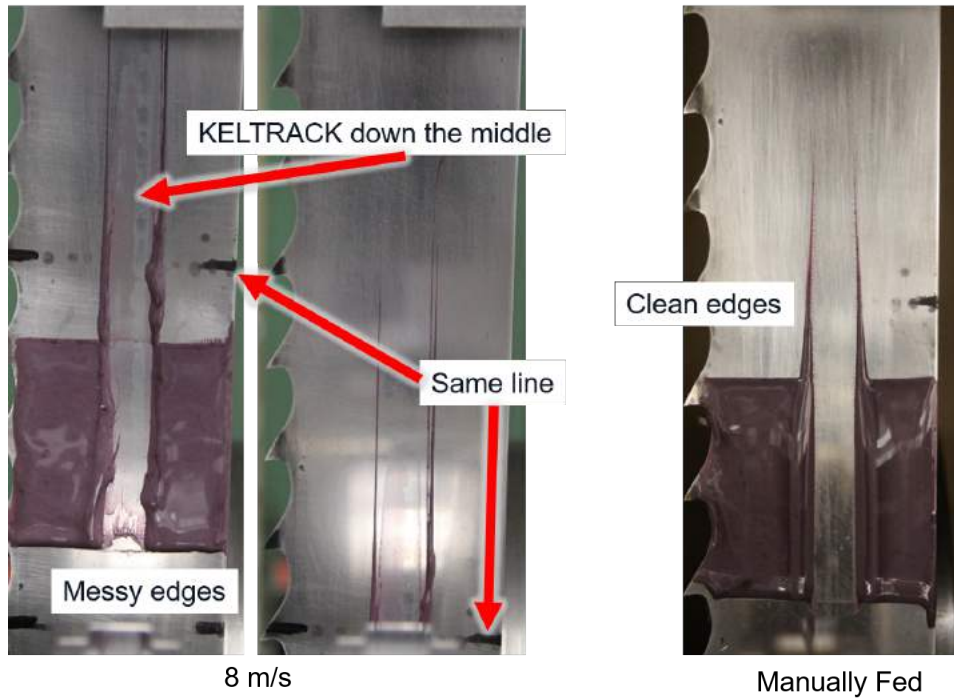


Figure 4.18: Interaction #0 (ambient light): The rail at the first location where the wheel initially picks up KELTRACK®. The Rail is moving from top to bottom. The initial KELTRACK® patch is pushed so far that it stretches across two images for the 8 m/s test. This was not seen in the manually fed test.

### 4.3. Effect of Speed on LFM Carry-down

---

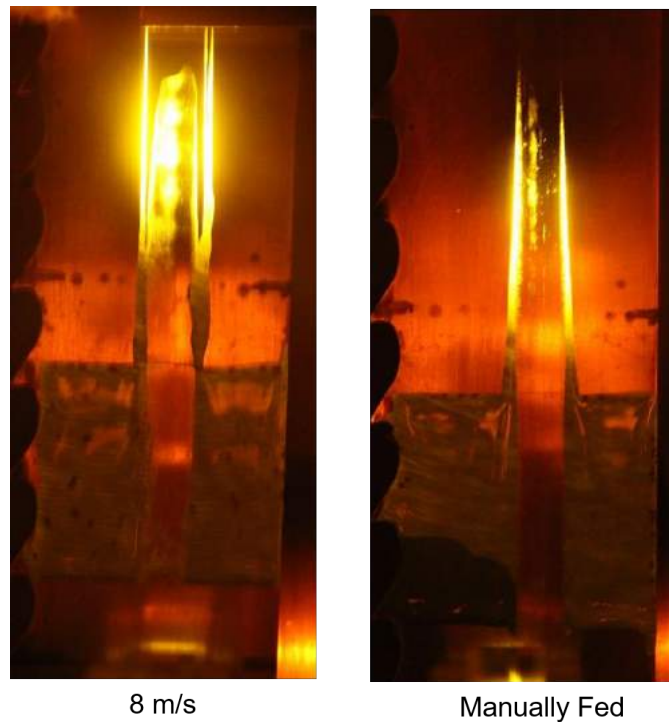


Figure 4.19: Interaction #0 (fluorescence): The rail at the first location where the wheel initially picks up KELTRACK®. The rail is moving from top to bottom.

In Figure 4.20 the results for interaction #1 (the first carry-down / first wheel to rail transfer) can be seen for both the 8 m/s and manually fed test. Three key observations about the 8 m/s test can be made in comparison to the manually fed test: 1) There is significantly more KELTRACK® down the centre contact patch in the 8 m/s test. 2) The edges of transferred KELTRACK® in the 8 m/s test are more non-linear. 3) The start of the transferred KELTRACK® is later than expected in the 8 m/s test. Using the number 1 written on the rail as a reference in the manually fed test KELTRACK® begins where expected based on the circumference of the wheel and the distance covered from interaction #0, but in the 8 m/s test it starts later than it should have.

### 4.3. Effect of Speed on LFM Carry-down

---

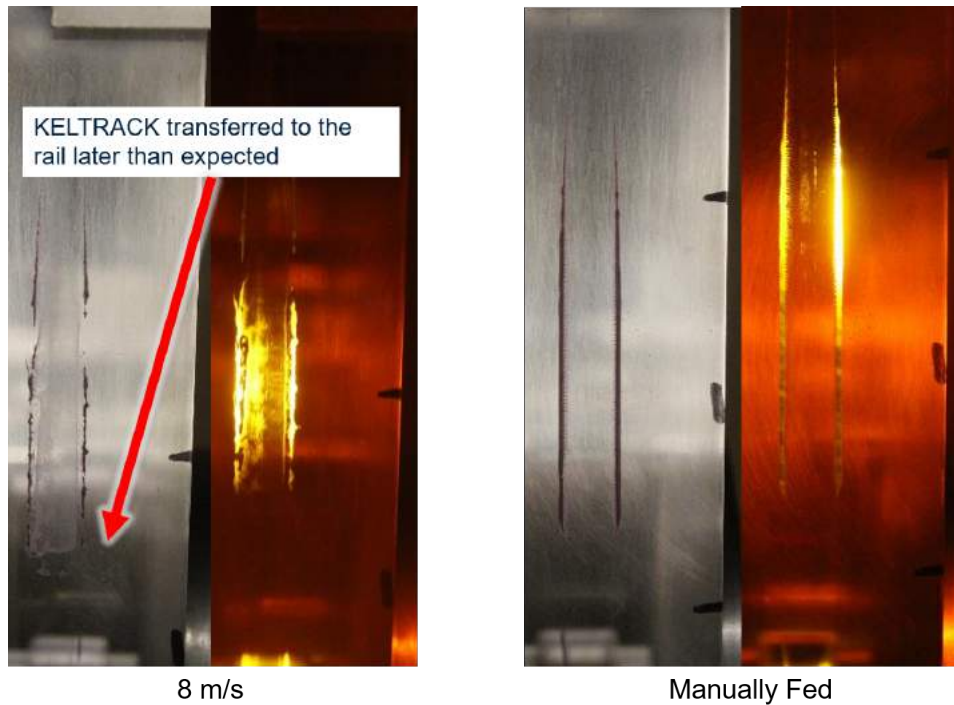


Figure 4.20: Interaction #1: Pictures in ambient light and fluorescence showing KELTRACK® transfer in both 8 m/s and manually fed test.

Figure 4.21 shows the results for interaction #3. The results are very similar to what was seen in interaction #1 with significantly more KELTRACK® transferred to the rail down the middle patch in the 8 m/s test being the most interesting observation. The starting point of KELTRACK® in the 8 m/s test is again seen to be later than was expected based on the circumference of the wheel and distance travelled.

Figure 4.22 shows the results for interaction #5. The results are similar to what was seen in earlier interactions but with a decrease in overall KELTRACK® transferred as is expected.

Figure 4.23 shows the results for the wheel after the experiment was finished (after 7 wheel/rail interactions) for both the 8 m/s and the manually fed test. There isn't an appreciable difference in the amount of KELTRACK® remaining on the wheel after each of the different tests.

4.3. Effect of Speed on LFM Carry-down

---

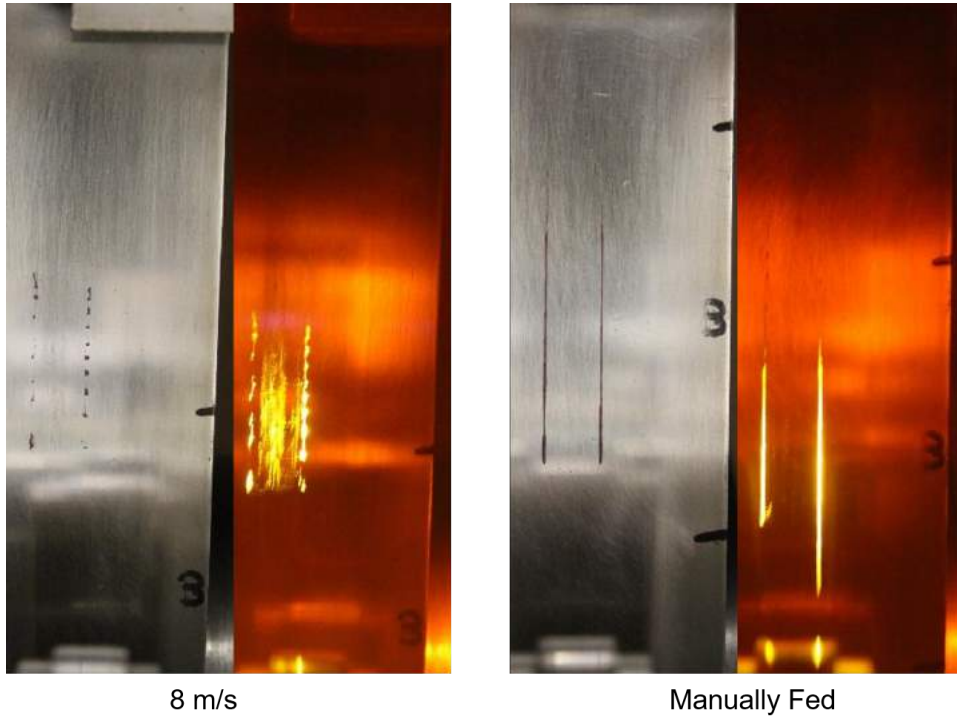


Figure 4.21: Interaction #3: Pictures in ambient light and fluorescence showing KELTRACK® transfer in both 8 m/s and manually fed test.

4.3. *Effect of Speed on LFM Carry-down*

---

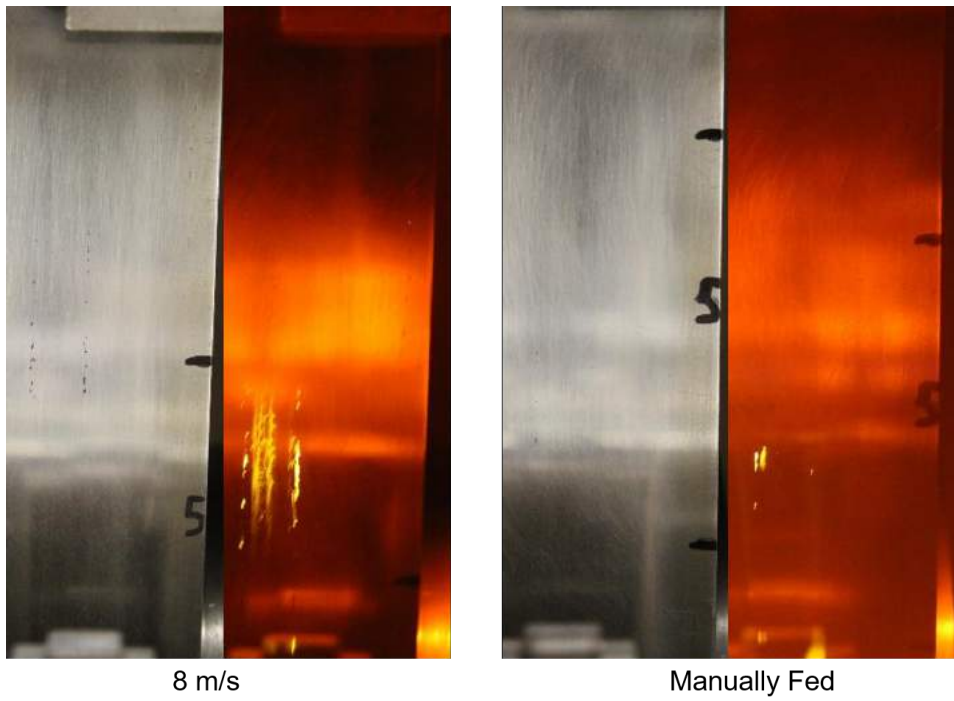


Figure 4.22: Interaction #5: Pictures in ambient light and fluorescence showing KELTRACK® transfer in both 8 m/s and manually fed test.

### 4.3. Effect of Speed on LFM Carry-down

---

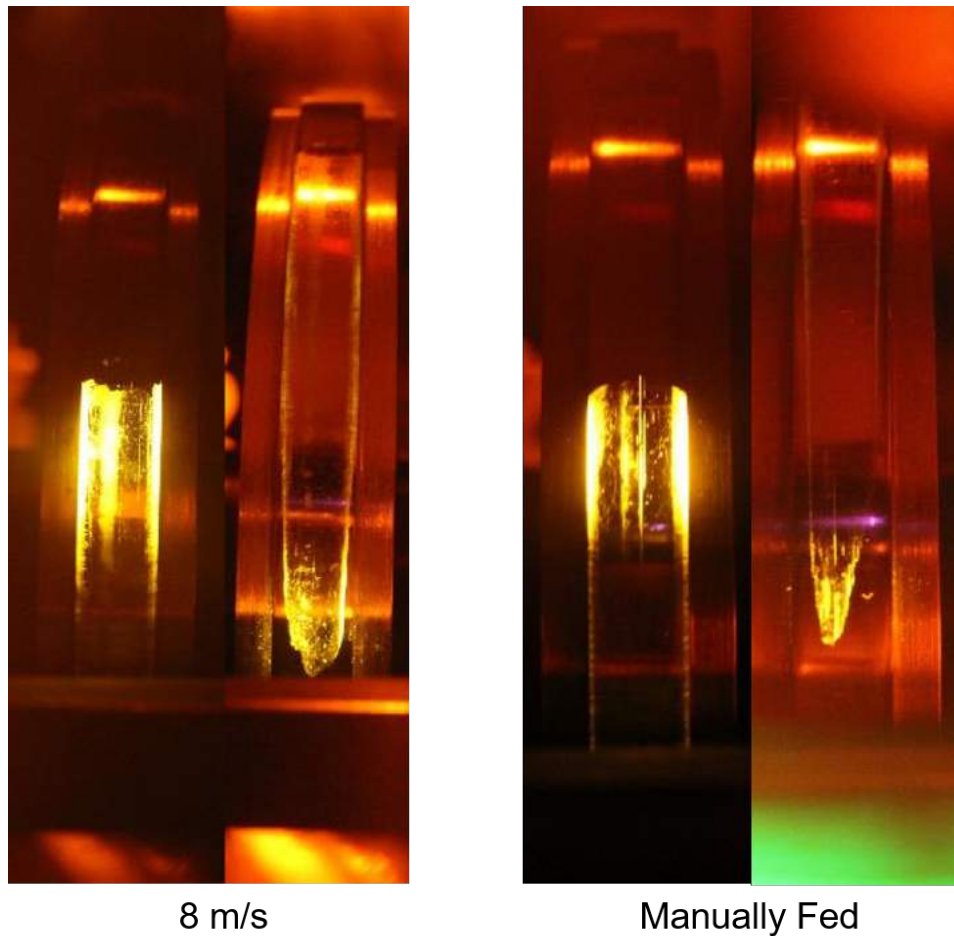


Figure 4.23: Wheel at the end of the experiment: Pictures in fluorescence showing KELTRACK® transfer in both 8 m/s and manually fed test. No noticeable difference can be seen with product coverage on the wheels at the conclusion of each test.

In conclusion, the role of speed does appear to have an effect on the carry-down behaviour of KELTRACK®. Tests were conducted at a manually fed speed and at 8 m/s. The 8 m/s test showed more KELTRACK® carry-down in the middle high pressure area of the wheel/rail interaction and there was more KELTRACK® present on the rail in the later interactions. In the 8 m/s test the KELTRACK® product was pushed further along the rail during the initial wheel/rail interaction (interaction #0). In addition

the KELTRACK® product started its wheel to rail transfer location later than expected and the low pressure edges were not as clean in comparison to the manually fed tests. The coverage of product on the wheel was not noticeably different between the two tests.

#### 4.4 Effect of Pressure on LFM Carry-down

The purpose of this experiment was to explore the effect of pressure on the carry-down of KELTRACK®. All previous experiments were run at an operating pressure of 25 psi which represents  $\sim 1/4$  full train pressure. The results of the 8 m/s speed test showed the presence of KELTRACK® down the middle patch of the wheel/rail contact interface. This was in contrast to lower speed tests where no KELTRACK® down the middle patch was observed. It was hypothesized that due to the increased speed the wheel was not in solid contact with the rail because the layer of film at this interface had increased. Since previous experiments were all conducted at 25 psi, an experiment to see the effect of pressure was designed. For this experiment three tests at 25 psi and 8 m/s were conducted and compared with one test at 50 psi ( $\sim 1/2$  full train pressure) and 8 m/s. The operational conditions are listed in Table 4.4. The wheel and the rail were set to the same speed. KELTRACK® was initially applied to the rail on a 50 mm long patch with a uniform height of 0.5 mm. In all the images for this experiment the rail is moving from top to bottom with respect to the page.

Speed (m/s)	8
Pressure 1 (psi)	25
Pressure 2 (psi)	50

Table 4.4: Speed and pressure conditions for the effect of pressure carry-down experiment.

Figure 4.24 shows the results of the rail after the first wheel/rail interaction where KELTRACK® is transferred from the rail to the wheel. The edges of KELTRACK® in the initial deposition patch are even more non-linear in the 50 psi test when compared to the 25 psi test. Other than this, not much difference is observed. Figure 4.25 shows the results viewed in fluorescence.

#### 4.4. Effect of Pressure on LFM Carry-down

---

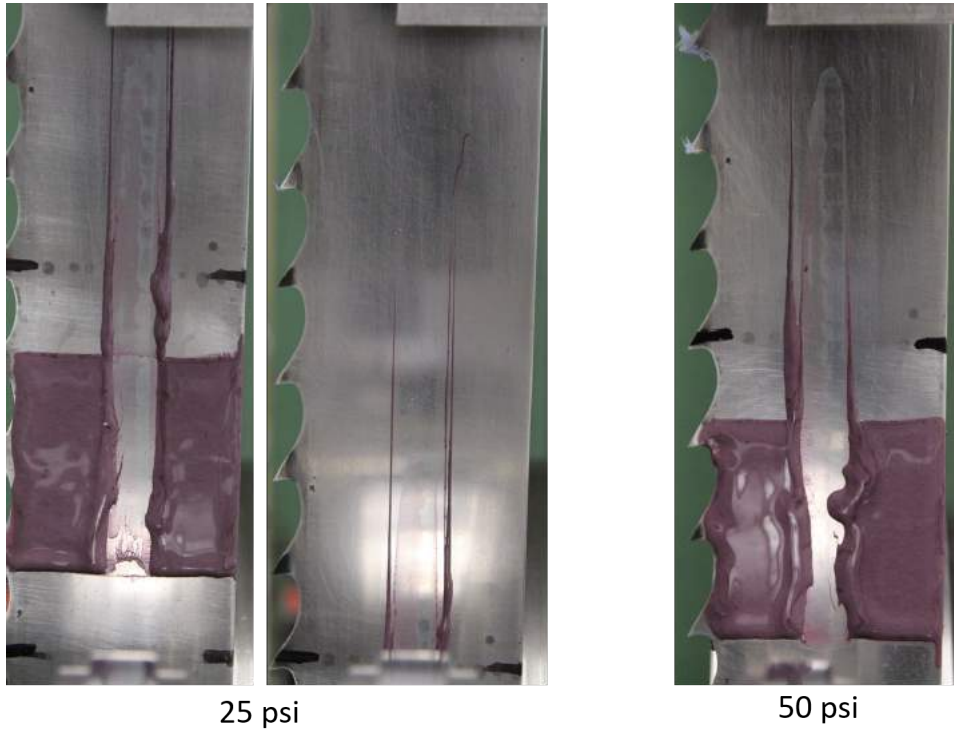


Figure 4.24: Interaction #0 (ambient light): The rail at the first location where the wheel initially picks up KELTRACK®. The rail is moving from top to bottom.

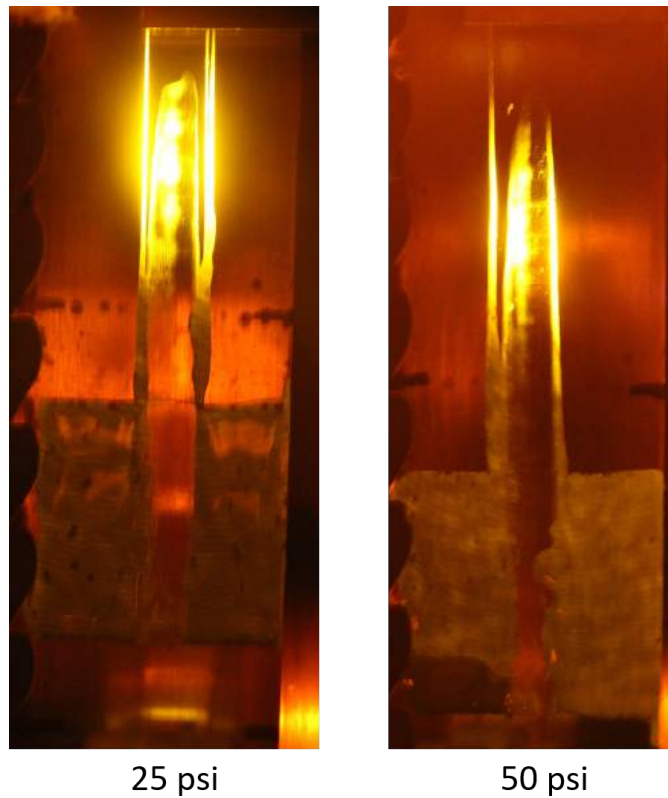


Figure 4.25: Interaction #0 (fluorescence): The rail at the first location where the wheel initially picks up KELTRACK®. The rail is moving from top to bottom.

Figure 4.26 shows the comparison of the first wheel to rail product transfer (interaction #1) for the two pressures studied. There is no clear observable difference in the amount of KELTRACK® transferred at this interaction however the wheel to rail transfer does begin earlier in the 50 psi case compared with the 25 psi test. The initial product deposition occurs much closer to when was expected based on the wheel circumference and distance travelled.

At interaction #3 some difference is seen in the amount of KELTRACK® transferred from the wheel to rail. There is slightly less KELTRACK® transferred in the 50 psi test when compared to the 25 psi test (Figure 4.27). This slight difference in transferred KELTRACK® is seen again at interaction #5 (Figure 4.28).

#### 4.4. Effect of Pressure on LFM Carry-down

---

No observable difference is seen when comparing the remaining product on the wheel after the 25 psi and 50 psi tests (Figure 4.29).

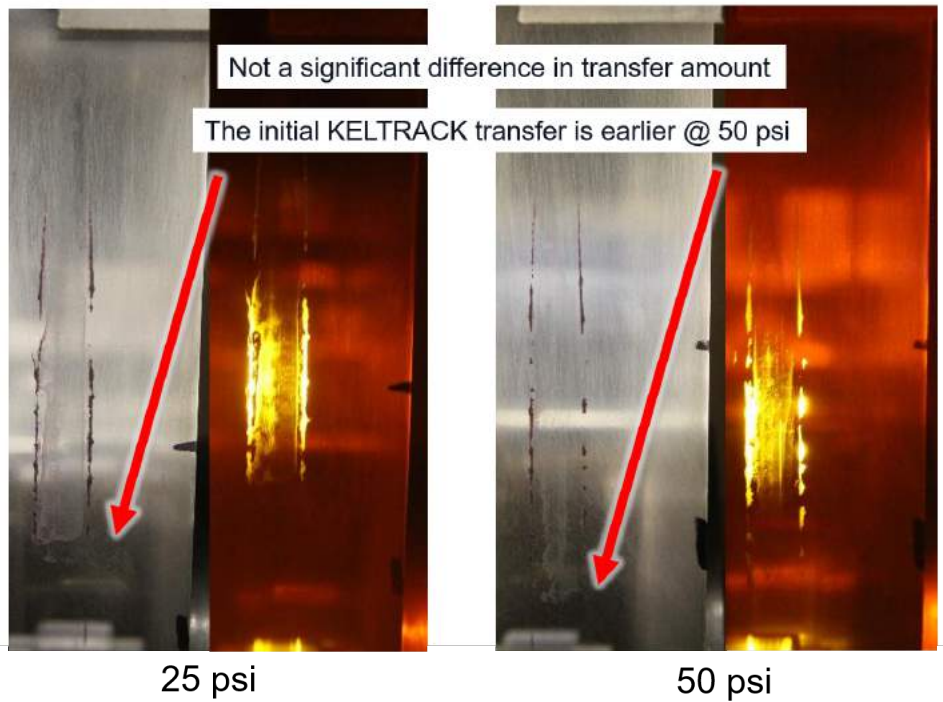


Figure 4.26: Interaction #1 (ambient & fluorescence): The first wheel to rail transfer location.

4.4. *Effect of Pressure on LFM Carry-down*

---

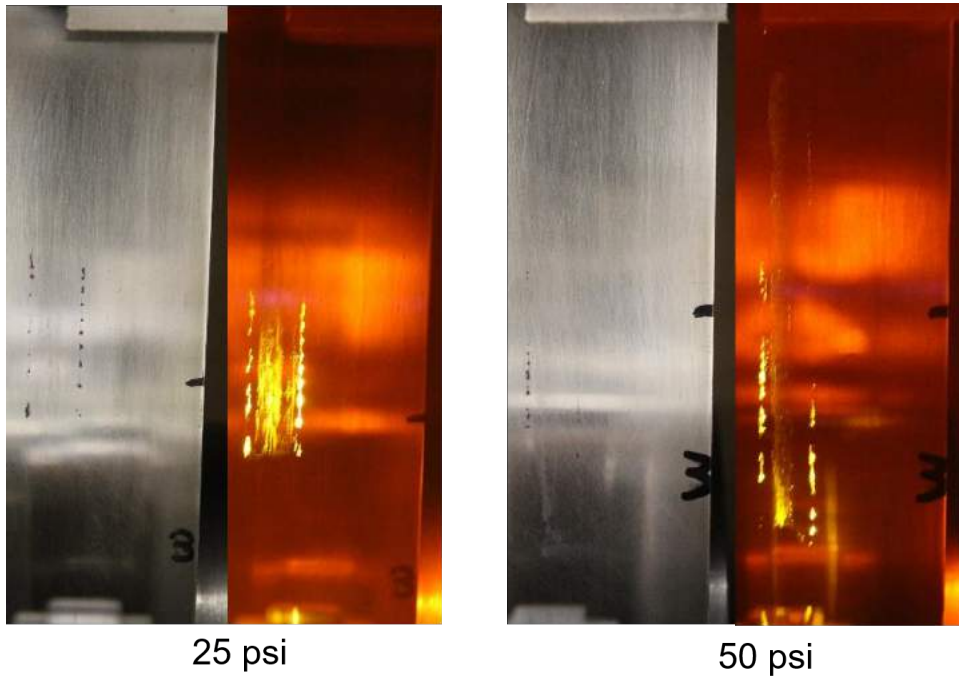


Figure 4.27: Interaction #3 (ambient & fluorescence): The third wheel to rail transfer location.

4.4. *Effect of Pressure on LFM Carry-down*

---

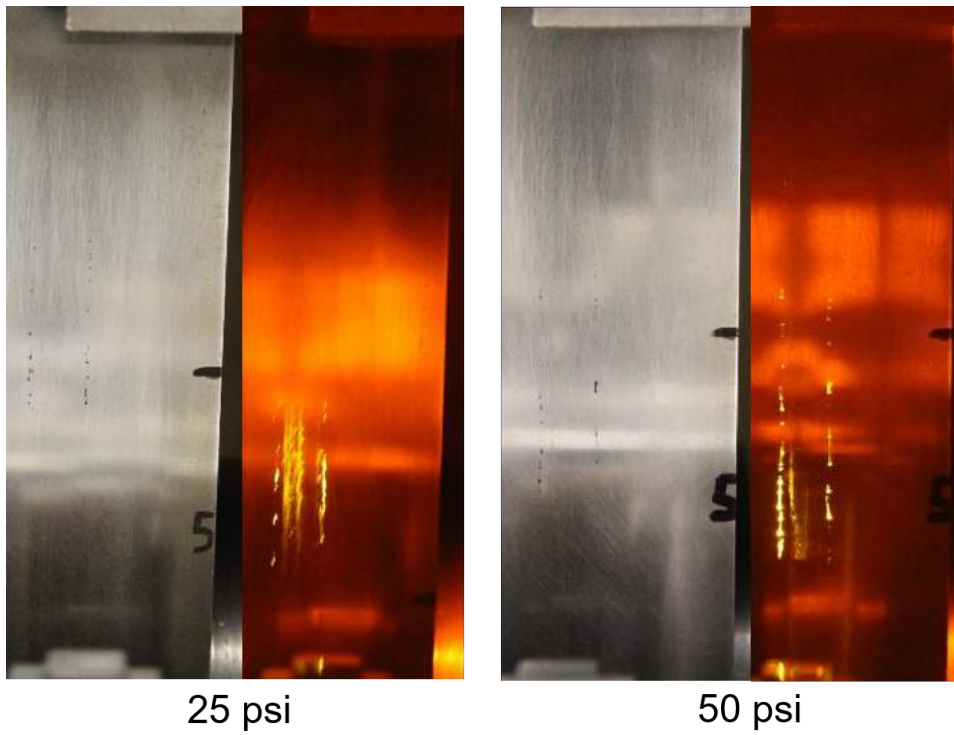


Figure 4.28: Interaction #5 (ambient & fluorescence): The fifth wheel to rail transfer location.

#### 4.4. Effect of Pressure on LFM Carry-down

---

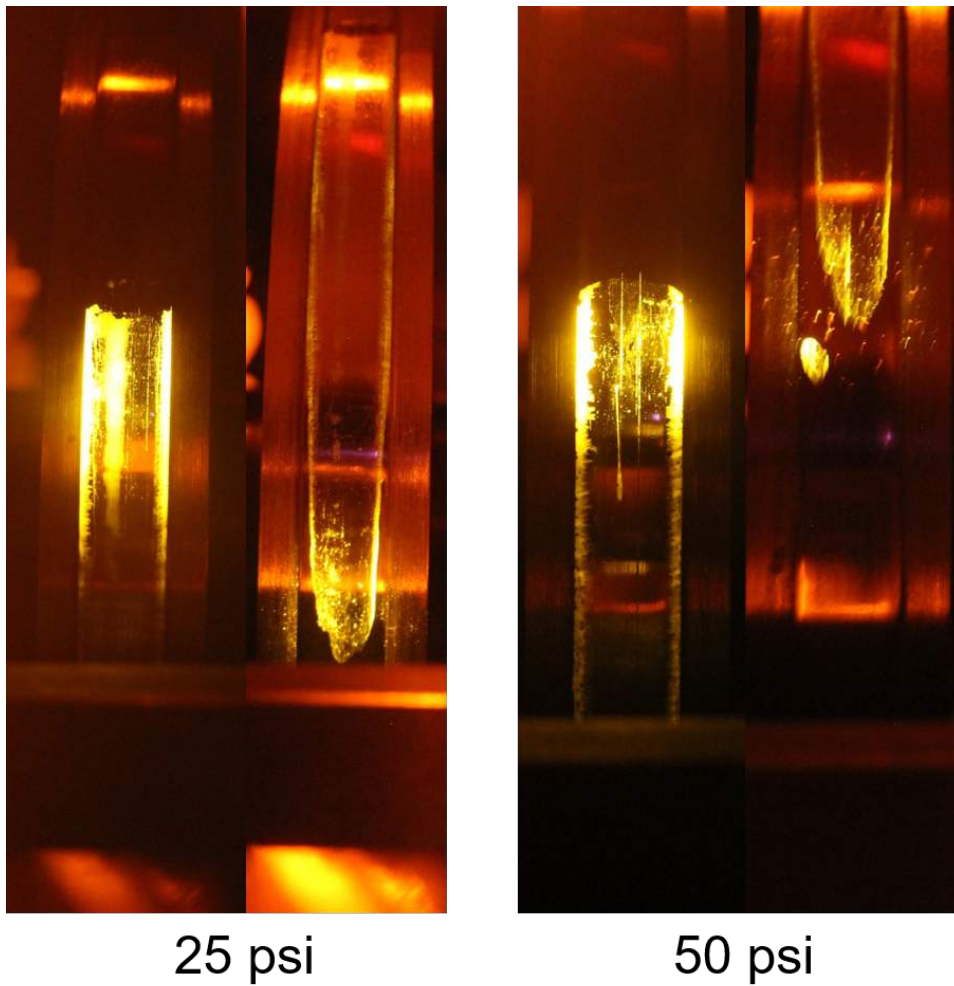


Figure 4.29: Wheel at the end of the experiment: Pictures in fluorescence showing the remaining KELTRACK® transfer in the 25 psi and 50 psi tests.

In conclusion, the role of pressure appears to potentially have an effect on the carry-down behaviour of KELTRACK®. Increasing the pressure reduces the amount of product initially transferred from the rail to the wheel, but further tests are required before this can be conclusively stated.

# Chapter 5

## Discussion of Results

The primary purpose of all the designed experiments was to validate the machines potential capability for answering the research questions outlined initially. The secondary purpose was to gain some insight into these research questions that could help guide the direction of future experiments which will answer these questions in a more quantitative and definitive manner, as these early experiments were all qualitative in nature.

With using a scaled wheel it is important to consider the impact of wheel scaling on centrifugal forces (Equation 5.1). In the experiments that were run, the surface speed could potentially match what was seen by a full scale train, but because we are using a 1/5th scale wheel, the centrifugal forces acting on the product could be up to 5x greater than what would be seen on a full scale train.

$$F_c = m \frac{v^2}{r} \quad (5.1)$$

This potential effect should be kept in mind when analysing results on this scaled machine.

### 5.1 Initial LFM Carry-down Experiments Discussion

Initially when the wheel was machined it was done such that the surface of the wheel was trued with respect to the axis of rotation. After the initial product carry-down experiments it was observed that the wheel had actually become crowned. The crowning most likely occurred during the machine commissioning process as the rail was initially curving under the applied pressures and could have created this wear pattern on the wheel.

After observing the results from the initial product carry-down experiments it was hypothesized that this unintended crowning could provide additional information that wouldn't have been gained with a trued wheel profile. The hypothesis was that as the wheel rolled through the initial

### 5.1. Initial LFM Carry-down Experiments Discussion

---

KELTRACK® patch the product would be squeezed out of the high pressure region and only the low pressure regions would pick up product (Figure 5.1b). The wheel would then transfer some of this wet product back onto the rail, but eventually what was left on the wheel would dry and remain on the wheel. When the train then enters a curved section of rail the bogie shifts and now a different part of the wheel experiences high pressure contact with the rail. Now there is a layer of dried KELTRACK® in the 3rd body layer between the wheel and rail providing added frictional benefits since the product is no longer squeezed out from this interaction region (Figure 5.1c). Because of this hypothesis, the wheel was not re-machined and further experiments were run using this crowned wheel profile.

In reality the bogie does experience some lateral shifting even along straight portions of track so the product in the low pressure regions might not have as much time to dry as is hypothesized before experiencing the full train pressure.

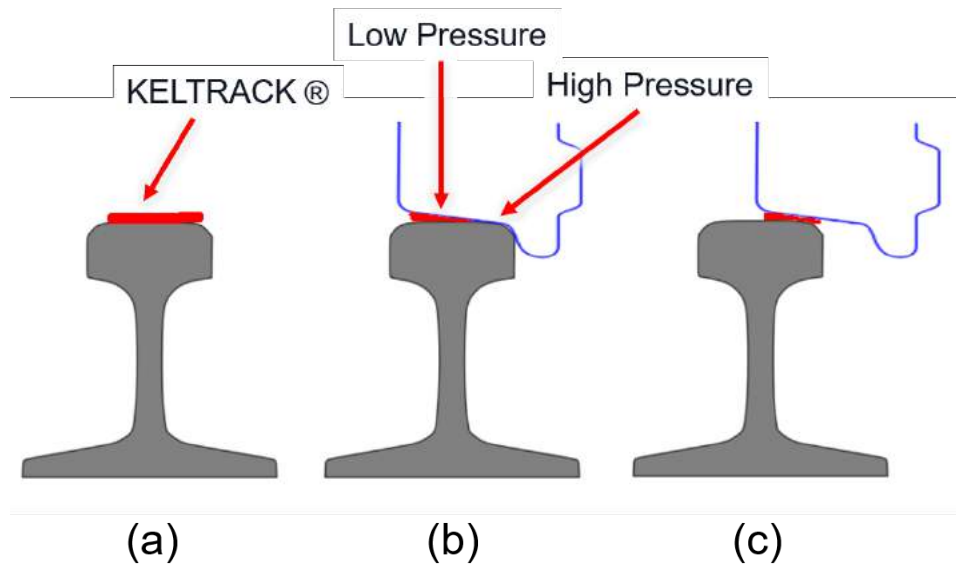


Figure 5.1: (a) Rail showing initial application of KELTRACK®. (b) Wheel/rail interaction along a straight section of track showing the location that KELTRACK® is picked up by the wheel. (c) Wheel/rail interaction along a curved section of track.

100 psi of applied pressure results in approximately full scale train load and in this experiment we only applied 25 psi of air pressure resulting in  $\sim 1/4$

full load. At speeds of 1 m/s (full train speed  $\sim 16$  m/s), this pressure was enough to squeeze the KELTRACK® out laterally from the main wheel/rail contact patch. The product was only picked up along the low pressure edges of the wheel. In addition the product was pushed forward in the direction of wheel travel resulting in the length of product coverage on the edges of the wheel being  $\sim 90$  mm (the original KELTRACK® patch on the rail was 50 mm). The wheel coverage ended up being longer than the initial applied patch.

Because of the crowning of the wheel (Figure 4.5), the resultant pressure at the contact patch would be slightly higher than initially predicted because the calculations were done with a 10 mm wide contact patch. Because our applied pressure for this experiment was so much lower than full scale pressure and the results showed that the product squeezed out, the difference in the resultant contact patch pressure was unimportant at this point in terms of the results seen.

Previously it was unclear how long the wet film transfer stage lasts for, how much product remains on the wheel and what the importance of dry film transfer is. The results from this initial experiment shows that this machine is capable of running experiments that could potentially answer these important questions.

## 5.2 Long Term LFM Carry-down Experiment Discussion

Where the other experiments tested the wet transfer behaviour of KELTRACK® in product carry-down, this experiment attempted to simulate what would happen to the carry-down behaviour of KELTRACK® that had dried (dry film transfer) on the wheel before being exposed to the full pressure at the wheel/rail interaction over a long distance.

The KELTRACK® was seen to wear faster in high pressure regions and remained longer in low pressure regions. At early stages in the wheel/rail transfer interaction it was seen that KELTRACK® was being transferred from the wheel to the rail and then picked up again by the wheel at locations different from the initial application site. The wheel/rail transfer had been observed before with wet KELTRACK® during the first 7 interactions, however this transfer of dried KELTRACK® after 287 wheel/rail interactions was new. Because the experiment ran continuously from 287 interactions to 1,715 interactions we can not say at which point exactly KELTRACK® was no longer being transferred from wheel to rail and vice versa. What we

### 5.3. Effect of Speed on LFM Carry-down Discussion

---

can say was that it was still happening after 287 interactions but then was no longer observable after 1,715 interactions and so presumably stopped at some point in that range. This experiment showed that dry KELTRACK® can be transferred from the wheel to rail and then back from the rail to wheel providing insight into something that was not previously well understood [17]. These distances refer to the distance the wheel has travelled on the machine. To relate this to a full scale train the number of interactions would stay the same but the distance would be scaled up 5x (Table 5.1). When analysing the results in relation to how they translate to a full scale train set-up, these scaled up distances need to be considered. One of the desired machine objectives was to be able to simulate up to 6 km of full scale wheel/rail interaction. The first three photos in Figure 4.8 show results from this desired range (the distances listed in the photo are machine distance). Future experiments focusing on this range with more observation stages could provide more insight.

# of Wheel/Rail Interactions	Machine Distance (m)	Full Scale Distance (m)
0	0	0
287	182	910
1,715	1,091	5,455
3,486	2,218	11,090
5,236	3,331	16,655
9,030	5,745	28,725

Table 5.1: Comparing experimental distances covered in the long term carry-down experiment with the full scale equivalent.

### 5.3 Effect of Speed on LFM Carry-down Discussion

Qualitatively there is noticeably more KELTRACK® present on the rail down the centre region of the wheel/rail interaction path for the 8 m/s test when compared to the manually fed test.

One potential explanation for this difference could be obtained from hydrodynamic lubrication theory. The schematic for a rotating cylinder on a flat plane is shown in Figure 5.2.

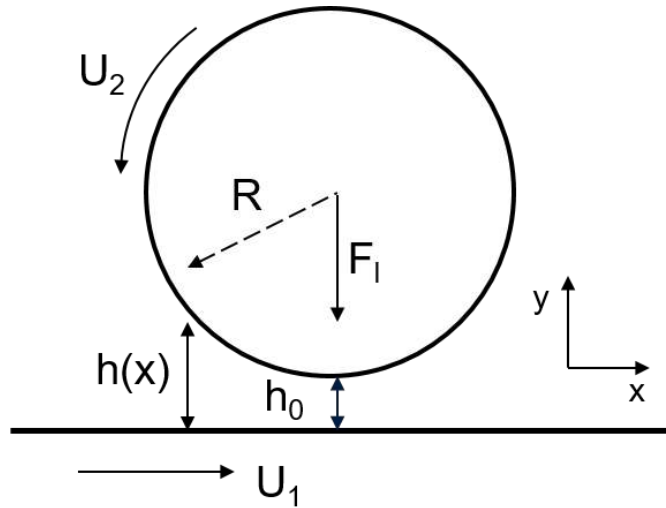


Figure 5.2: Schematic showing the important elements in hydrodynamic lubrication theory.

For the infinite cylinder-plane geometry, the Reynolds equation reduces to:

$$\frac{d}{dx} \left( \frac{h^3}{\mu} \frac{dp}{dx} \right) = 6U_m \frac{dh}{dx} \quad (5.2)$$

$$U_m = \frac{U_1 + U_2}{2} \quad (5.3)$$

where  $h$ ,  $p$ ,  $\mu$ ,  $U_m$  are hydrodynamic film thickness, pressure, viscosity and average sliding speed. The solution obtained by Martin in 1916 [11] states the following:

$$h_0 = 4.9 \frac{\mu U_m R}{F_l} \quad (5.4)$$

This solution shows us the relation between sliding speed and film thickness height in that an increase in sliding speed results in an increase in film thickness. This could be a possible explanation for why we saw greater carry-down when the speed of the experiments was increased but the applied pressure was kept constant. One key potential problem with this theory is that it was developed for a Newtonian fluid and we know the KELTRACK® product to be non-Newtonian, showing shear-thinning behaviour. We know

### 5.3. Effect of Speed on LFM Carry-down Discussion

---

that as the shear rate increases the viscosity of this LFM decreases, potentially countering the expected resultant effect of increased speed on the film thickness. This would have to be considered before trying to generate an accurate model.

At 8 m/s the start of the KELTRACK® at interaction #1 was further down the rail than geometrically predicted. This was not seen in the manually fed tests. It's hard to get the wheel and rail moving at the exact same speed, so potentially what we are seeing is the effect of creep (the rail is moving faster than the wheel in this case), however if this was the case one would expect to see this delay in KELTRACK® deposition propagating throughout the remaining interactions getting more pronounced each time, but this is not seen. Instead the starting deposit location for interactions #2 through #6 are consistent with respect to where interaction #1 started. If we go back to the hydrodynamic lubrication theory it's possible that there is some slipping between the wheel and rail at interaction #0 where KELTRACK® is initially transferred to the wheel, but after that there is metal on metal contact and the two surfaces move in unison. The effect is not seen as strongly for the remaining interactions because the thickness of the KELTRACK® on the wheel is considerably thinner than the initial application patch reducing the effects seen by hydrodynamic lubrication theory. This explanation of creep occurring could be confirmed in a repeat experiment using markers on the wheel and rail at interaction #0 along with the high-speed camera.

The amount of KELTRACK® remaining on the wheel was not noticeably different between the two speeds from a qualitative observation. One possible explanation is that regardless of the amount of KELTRACK® initially picked up, the only product remaining on the wheel after several wheel/rail interactions is in the low pressure zones on the wheel which doesn't experience full contact pressure, thus remaining on the wheel in these locations.

The results of this test showed that running experiments at only  $\sim 1/4$  full scale train pressure (25 psi) may be producing results that won't accurately reflect a full scale train setup. This provided the motivation to run experiments to determine the effect of pressure on product carry-down.

## 5.4 Effect of Pressure on LFM Carry-down Discussion

When increasing the pressure from 25 psi to 50 psi we see slightly less wheel to rail transfer of the product and this is more noticeable in the later interactions. The location of the product at each interaction in the 50 psi, 8 m/s test occurred closer to where expected and is more comparable to the location for the 25 psi, manually fed test. This is in contrast to the 25 psi, 8 m/s test where the location of transferred KELTRACK® on the rail occurred later than expected. Referring back to Equation 5.4 we see that an increase in applied load will result in a reduction of film thickness at the wheel/rail interaction, which should result in less product picked up by the wheel and less wheel to rail product transfer at later interactions. These initial experimental observations potentially agree with the hydrodynamic film lubrication theory mentioned earlier. However, this again does not take into account the viscosity-pressure dependence of the LFM, a property we currently do not know about with LFM used in these experiments.

Only one test at 50 psi was conducted at the time of writing so further experiments at 50 psi are required before reading too much into the results from this single test. Alternatively, increasing the pressure to 75 psi may be more beneficial in order to see a bigger difference in transfer amount before conclusively saying what effect pressure has on the carry-down of KELTRACK®.

## Chapter 6

# Conclusion

A new custom machine was designed and built for the purpose of testing the carry-down behaviour of liquid friction modifiers used in the freight train industry. The machine's design focused on the wheel/rail interaction zone and was built to 1/5 th the scale of a freight train so that testing could be run in a laboratory environment. The machine's design included several key features that were identified as potentially playing crucial roles in carry-down:

- Precise, full scale speed control from 0 m/s to 18 m/s (speed commonly seen in curved sections of freight rail).
- Independent speed control for the rail and wheel, which provides the ability to simulate creep (so that wheel/rail interaction can be simulated for both straight and curved track). The limitations for creep initiating have yet to be explored.
- Precise, full scale pressure control at the wheel/rail interface from 0 MPa to 1033 MPa.
- Ability to simulate multiple wheel/rail interactions replicating carry-down.
- Optical access to be able to the record film transfer at the wheel/rail interface.

Using a computer interface controller, the machine demonstrated the ability to perform multiple different experiments based on changing variables that demonstrated their effect on liquid friction modifier carry-down. The machine also demonstrated good repeatability among experiments when the control variables remained unchanged.

Fluorescence was used as a technique for visualizing deposited KELTRACK® that was otherwise too thin to be seen by the un-aided eye under ambient light conditions. Rhodamine-B was the fluorescent tracer that was added to the base KELTRACK® solution.

The speed of the wheel was shown to have an effect on the amount of initial transfer of LFM from the rail to the wheel. Experiments run at a manually fed speed showed that KELTRACK® was only transferred along the low pressure edges of the crowned wheel and was not transferred from the rail to the wheel at the centre full pressure region of the crowned wheel. Wet KELTRACK® was observed to be transferred from the wheel to the rail on ensuing wheel/rail interactions. Wheel to rail transfer was no longer observed after 5 interactions, but KELTRACK® still remained on the wheel along the low pressure edges. Experiments run at a speed of 8 m/s showed an increase in the amount of KELTRACK® transferred onto the wheel from the initial application patch on the rail. The increase in initial pickup was seen primarily in the high pressure centre region. This led to increased wheel to rail wet KELTRACK® transfer on ensuing wheel/rail interactions. Speed does not appear to have an effect on the resultant coverage of product on the wheel as there was no noticeable difference when comparing the wheels at the conclusion of each speed test.

The contact pressure of the wheel on the rail was shown to have an effect on the initial transfer of LFM from the rail to the wheel. Increasing the pressure at the wheel/rail interface was shown to reduce the amount of KELTRACK® that was initially transferred from the rail to the wheel, resulting in less wet KELTRACK® transfer from the wheel to rail on the ensuing wheel/rail interactions.

A long term carry-down test of 9,030 wheel/rail interactions showed that dry KELTRACK® is transferred from the wheel to the rail and then is transferred from the rail back to the wheel at later interactions. This demonstrated the potential for a leading train wheel to transfer product to the rail that is then later picked up by trailing wheels potentially resulting in greater KELTRACK® application efficiency and less product wastage. KELTRACK® was shown to visibly remain on the wheel after simulating almost 6 km of wheel/rail interactions.

The carry-down tests performed thus far were primarily qualitative in nature, focusing on the validating the machine's capabilities and providing guidance for future experiments. A quantitative method for measuring the amount of product present on the wheel or the rail would make it possible to develop a model relating the amount of product carry-down to the experimental conditions (speed, pressure, number of interactions). The effect of pressure was only briefly explored and requires further experimentation before any conclusions can be made. Other factors such as wheel profile,

temperature and material characteristics could all play a role in product carry-down and have yet to be explored. It is recommended that field trials are also conducted to validate that what is seen in the laboratory findings.

## 6.1 Recommended Changes to Machine

Below is a list of improvements I would recommend be made to the machine:

- The speed sensor that measures the rail speed is located such that it detects the holes that pass by on the band saw wheel that has an adjustable tilt angle for when the user adjusts the blade tension. This results in needing to adjust the position of the sensor every time the blade is adjusted so that the sensor works correctly. I would recommend that the sensor is moved to the second band saw wheel that is not adjustable.
- The speed sensor on the wheel shaft relies on 1 notch in the wheel shaft. I would swap this out for a different technology if finer speed measurement is required. The same recommendation applies to the speed sensor that is measuring the rail speed. Neither set-up currently accurately measure brief instantaneous changes in speed and is better suited for measuring average speed of a period of time.
- The current band saw blade is only 2" wide and once the blade runs steady, it's location is not what was expected when designing the mounting locations for the train wheel. As a result, the wheel had to be shifted slightly off centre along the rotating shaft in order to make contact with the rail. Using a wider blade would allow for the train wheel to be perfectly centred between to the two mounting brackets where the force is applied.
- The way the software controller is written, motor speeds are changed in increments of 0.3 to 0.4 Hz. The VFD's are capable of changing the speeds in increments as low as 0.1 Hz. The software controller and extra electronics could be re-worked so that finer speed control is achieved.

# Bibliography

- [1] H. Chen, S. Fukagai, Y. Sone, T. Ban, and A. Namura. Assessment of lubricant applied to wheel / rail interface in curves. *Wear*, 314:228–235, 2014.
- [2] K. Conn. Wayside top-of-rail (tor) friction control performance. September 27, 2005.
- [3] J. Cotter, D.T. Eadie, D. Elvidge, N. Hooper, J. Robert, T. Makowsky, and Y. Liu. Top of rail friction control: Reductions in fuel and greenhouse gas emissions. *2005 Conference of the International Heavy Haul Association*, pages 327–334, 2005.
- [4] J. Cotter, D. Elvidge, Y. Liu, and J. Roberts. Utilization of top of rail friction modifiers to reduce greenhouse gas emissions for the freight railroad industry, 2004.
- [5] D.J. Coyle, C.W. Macosko, and L.E. Scriven. Film-splitting flows in forward roll coating. *J. Fluid Mech*, 171:183–207, 1986.
- [6] D.T. Eadie, E. Bovey, and J. Kalousek. The role of friction control in effective management of the wheel/rail interface. pages 432–481, 2002.
- [7] D.T. Eadie, L. Maglalang, B. Vidler, D. Lilley, and R. Reiff. Trackside top of rail friction control at cn. *2005 Conference of the International Heavy Haul Association*, pages 85–92, 2005.
- [8] D.T. Eadie, K.D. Oldknow, L. Maglalang, T. Makowsky, R. Reiff, P. Sroba, and W. Powell. Implementation of wayside top of rail friction control on north american heavy haul freight railways. *The Seventh World Congress on Railway Research*, June 2006.
- [9] M. Harmon and R. Lewis. Review of top of rail friction modifier tribology. *Tribology - Materials, Surfaces Interfaces*, 10:3:150–162, 2016.

- [10] N.E. Hooper, D.T. Eadie, B. Vidler, and T.W. Makowsky. Top of rail friction control: Lateral force and rail wear reduction in a freight application. *International Heavy Haul Specialist Technical Session Proceedings*, pages 5.73–5.80, May 2003.
- [11] H.M. Martin. Lubrication of gear teeth. *Engineering (London)*, 102:119–121, 1916.
- [12] M. Naeimi, Z. Li, and R. Dollevoet. Scaling strategy of a new experimental rig for wheel-rail contact. *International Journal of Mechanical, Aerospace, Industrial and Mechatronics Engineering*, 8, 2014.
- [13] K. Oldknow, D.T. Eadie, and R. Stock. The influence of precipitation and friction control agents on forces at the wheel/rail interface in heavy haul railways. *J Rail and Rapid Transit*, 227:86–93, 2012.
- [14] H. Rahmani. Keltrack detection method. Information was communicated verbally.
- [15] M. Roney, P. Sroba, K.D. Oldknow, and R. Dashko. Canadian pacific railway 100 2005 *Conference of the International Heavy Haul Association*, pages 93–102, 2005.
- [16] L. Stanlake. Film splitting of liquid friction modifier formulations in the wheel-rail contact, October 2012.
- [17] R. Stock, D. Elvidge, L. Stanlake, J. VanderMarel, and J. Cotter. Research objectives and carry-down machine design requirements. Information was communicated verbally over a period of several meetings.
- [18] R. Stock, K. Oldknow, D. Mitchell, and J. VanderMarel. Top of rail friction control for heavy haul: Status and opportunities. 24–26 November 2015.
- [19] Y. Suda, T. Iwasa, H. Komine, T. Fuji, K. Matsumoto, N. Ubukata, T. Nakai, M. Tanimoto, and Y. Kishimoto. The basic study on friction control between wheel and rail (experiments by test machine and scale model vehicle),. volume II, page 343348, 2003.
- [20] P. Temple, M. Harmon, R. Lewis, M. Burstow, and B. Temple. Optimisation of grease application to railway track. *The Third International Conference on railway technology: research, development and maintenance*, pages 1–16, 2016.
- [21] E. Terpetschnig, Y. Povrozin, and J. Eichorst. Polarization standards.

# Appendix A

## Experimental Procedure

### A.1 Pre Run Checklist

1. Ensure that the wheel and rail are properly cleaned and free of any previous test sample material. DO NOT clean the blade while the machine is running.
2. Ensure that the band saw table is clear of any tools or debris.
3. Is the V-belt properly tensioned?
4. The center knob on the top wheel of the band saw comes loose after operation. Use the custom tool inside the door to ensure it is properly tight.
5. Make sure the blade is properly centered on the wheel.
6. Drain the water out of the main air supply line.

### A.2 Test Procedure

1. Open up the main air supply line and the manual valve that leads through the filter to the pressure regulator. Adjust the regulator to the pressure that you want to apply. Open up manual valve adjacent to the regulator to allow air to flow to the solenoid valves.
2. Switch on the two motor main power switches.
3. Open up the LabVIEW controller program.
4. Click the motor enable buttons to activate the VFDs.
5. Using the speed controls, adjust the speeds of the Wheel and Rail motors to the desired level.
6. Once desired speeds are achieved, turn off the motors using the motor enable buttons in the LabVIEW controller.

### *A.3. Normal Shut Down Procedure*

---

7. Apply the product to the designated location on the rail.
8. Click the motor enable buttons.
9. Click “Run Test”. The test will now automatically run. The wheel will automatically engage onto the rail and disengage when the experiment is done.
10. When the Wheel has disengaged from the Rail, click the “Stop” button to end the program.

### **A.3 Normal Shut Down Procedure**

1. Turn off both motor switches and lock out the switches using the lockout locks.

## Appendix B

# Hertzian Contact Patch Calculations

When two bodies with curved surfaces are in contact under a force, the line contact changes to an area contact and 3 dimensional stresses are developed. These stresses are contact stresses, the contact pressure can be modelled using a Hertzian contact stress theory.

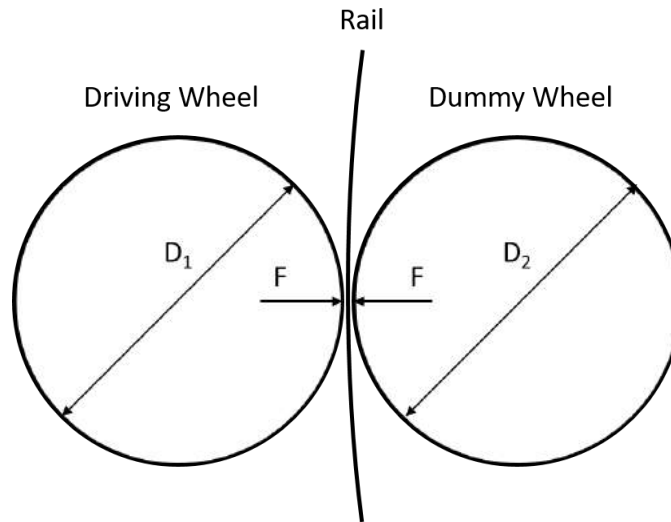


Figure B.1: Hertzian contact model schematic of two cylinders.

$$P_{max} = \frac{2F}{\Pi b l} \quad (\text{B.1})$$

$$b = \sqrt{\frac{2F}{\pi l} \frac{(1 - \nu_1)^2/E_1 + (1 - \nu_2)^2/E_2}{1/d_1 + 1/d_2}} \quad (\text{B.2})$$

$P_{max}$  = Contact pressure

## Appendix B. Hertzian Contact Patch Calculations

---

$\nu$  = Poisson's ratio

$E$  = Elastic modulus

$d$  = Diameter of object

$F$  = Applied force

$l$  = Line contact length

The components are all made out of a mild steel and the following values were used:

$\nu = 0.30$

$E = 207 \text{ GPa}$

$d = 190 \text{ mm}$

$F = 3150 \text{ lbf (14 kN)}$

$l = 10 \text{ mm}$

Using the above values in equations B.1 and B.2 results in an estimated contact pressure of **1033 MPa** at the wheel/rail interaction site.

## Appendix C

# Control Circuitry Schematic

The details of the control circuitry shown in section 2.2.6 is presented here. Two LM234 low power quad operational amplifiers are used, one for each VFD as each VFD requires 3 signals to be boosted. A non-inverting configuration is used for each signal, the schematic is shown in Figure C.1. Equation C.1 is the gain achieved when using this configuration.

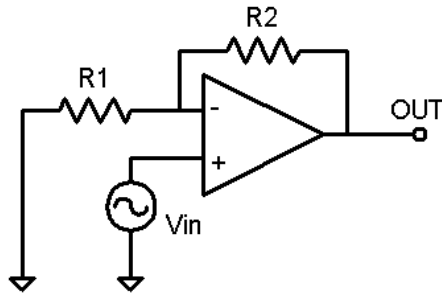


Figure C.1: Non-inverting op amp configuration.

$$V_{out} = V_{in} \left( 1 + \frac{R_2}{R_1} \right) \quad (C.1)$$

$V_{in} = 3V$  in this equation. The Lenz VFD signal boost uses values of  $R_2 = 10K\Omega$  and  $R_1 = 3.8K\Omega$  for a gain of 3.6, resulting in  $V_{out} = 10V$ . The Baldor VFD signal boost uses values of  $R_2 = 33K\Omega$  and  $R_1 = 3.8K\Omega$  for a gain of 9.5, resulting in  $V_{out} = 28V$ .